Made available by Hasselt University Library in https://documentserver.uhasselt.be

Identification of a 5-Plex Cytokine Signature that Differentiates Patients with Multiple Systemic Inflammatory Diseases

Peer-reviewed author version

Hoste, Levi; Meertens, Bram; OGUNJIMI, Benson; Sabato, Vito; Guerti, Khadija; VAN DER HILST, Jeroen; BOGIE, Jeroen; Joos, Rik; Claes, Karlien; Debacker, Veronique; Janssen , Fleur; Tavernier, Simon J.; Jacques, Peggy; Callens, Steven; Dehoorne, Joke & Haerynck, Filomeen (2024) Identification of a 5-Plex Cytokine Signature that Differentiates Patients with Multiple Systemic Inflammatory Diseases. In: Inflammation,.

DOI: 10.1007/s10753-024-02183-3
Handle: http://hdl.handle.net/1942/44703

Title page

Manuscript title: Identification of a 5-plex cytokine signature that differentiates patients with multiple systemic inflammatory diseases

Authors: Levi Hoste[1,2], Bram Meertens[1,2], Benson Ogunjimi[3,4,5,6,7], Vito Sabato[8], Khadija Guerti[9], Jeroen van der Hilst[10,11], Jeroen Bogie[12,13], Rik Joos[4,8,14], Karlien Claes[1,2], Veronique Debacker[1], Fleur Janssen[15], Simon J Tavernier[1,16,17,18], Peggy Jacques[19], Steven Callens[20], Joke Dehoorne[14], Filomeen Haerynck[1,2]

Affiliations:

[1]Primary Immune Deficiency Research Laboratory, Department of Internal Diseases and Pediatrics, Centre for Primary Immunodeficiency Ghent, Jeffrey Modell Diagnosis and Research Centre, Ghent University, Ghent, Belgium;

[2]Department of Internal Medicine and Pediatrics, Division of Pediatric Pulmonology, Infectious Diseases and Inborn Errors of Immunity, Ghent University Hospital, European Reference Network for Rare Immunodeficiency, Autoinflammatory and Autoimmune Diseases Network (ERN-RITA) Center, Ghent, Belgium;

[3]Rheumatology Department, Antwerp Hospital Network, Antwerp, Belgium;

[4]Division of Pediatric Rheumatology, Antwerp University Hospital, Edegem, Belgium;

[5]Antwerp Center for Pediatric Rheumatology and Autoinflammatory Diseases, Antwerp, Belgium;

[6]Division of Pediatric Rheumatology, Brussels University Hospital, Jette, Belgium;

[7]Antwerp Center for Translational Immunology and Virology (ACTIV), Centre for Health Economics Research and Modeling Infectious Diseases (CHERMID), Vaccine and Infectious Disease Institute (VAXINFECTIO), University of Antwerp, Antwerp, Belgium

[8]Department of Immunology, Allergology, and Rheumatology, Antwerp University Hospital, Edegem, Belgium;

[9]Department of Clinical Chemistry, Antwerp University Hospital, Edegem, Belgium;

[10]Department of Infectious Diseases and Immune Pathology, Jessa General Hospital, Hasselt, Belgium

[11]Limburg Clinical Research Center, Hasselt University, Hasselt, Belgium;

[12]Department of Immunology and Infection, Biomedical Research Institute, Hasselt University, Hasselt, Belgium;

[13]University MS Centre, Hasselt University, Hasselt, Belgium;

[14]Department of Pediatric Rheumatology, Ghent University Hospital, European Reference Network for Rare Immunodeficiency, Autoinflammatory and Autoimmune Diseases (ERN-RITA) Center, Ghent, Belgium;

[15]Faculty of Medicine and Health Sciences, Ghent University, Ghent, Belgium;

[16]Center for Medical Genetics, Ghent University Hospital, Ghent, Belgium;

[17]Department of Biomedical Molecular Biology, Ghent University, Ghent, Belgium;

[18]Unit of Molecular Signal Transduction in Inflammation, VIB-UGent Center for Inflammation Research, Ghent, Belgium;

[19]Department of Rheumatology, University Hospital Ghent, Ghent, Belgium;

[20]Department of General Internal Medicine, Ghent University Hospital, Ghent, Belgium;

Corresponding author: Filomeen Haerynck, Ghent University Hospital, Corneel Heymanslaan 10, 9000 Gent, +32 9 332 35 81, filomeen.haerynck@uzgent.be

Conflict of interest: The authors have declared that no conflict of interest exists.

Abstract

Patients with non-infectious systemic inflammation may suffer from one of many diseases, including hyperinflammation (HI), autoinflammatory disorders (AID), and systemic autoimmune disease (AI). Despite their clinical overlap, the pathophysiology and patient management differ between these disorders. We aimed to investigate blood biomarkers able to discriminate between patient groups. We included 44 patients with active clinical and/or genetic systemic inflammatory disease (9 HI, 27 AID, 8 systemic AI) and 16 healthy controls. We quantified 55 serum proteins and combined multiple machine learning algorithms to identify five proteins (CCL26, CXCL10, ICAM-1, IL-27, and SAA) that maximally separated patient groups. High ICAM-1 was associated with HI. AID was characterized by an increase in SAA and decrease in CXCL10 levels. A trend for higher CXCL10 and statistically lower SAA was observed in patients with systemic AI. Principal component analysis and unsupervised hierarchical clustering confirmed separation of disease groups. Logistic regression modelling revealed a high statistical significance for HI ($P=0.001$), AID, and systemic AI ($P<0.0001$). Predictive accuracy was excellent for systemic AI (AUC 0.94) and AID (0.91) and good for HI (0.81). Further research is needed to validate findings in a larger prospective cohort. Results will contribute to a better understanding of the pathophysiology of systemic inflammatory disorders and can improve diagnosis and patient management.

Introduction

Inflammation provides essential protective measures for the human body and occurs in response to stress or damage [1,2]. It is a prerequisite to ensure the removal of detrimental stimuli, as well as to initiate the healing of damaged tissues and cells. The inflammatory response is pathological when it occurs persistently or is exaggerated, which can occur in the presence or absence of a pathogen [3]. Caring for patients with acute, chronic, or relapsing systemic inflammation is challenging, especially because their clinical presentations can appear similar, despite having diverse underlying causes.

Autoinflammatory disorders (**AID**) are a rapidly expanding group of diseases that present recurrent or continuous systemic inflammation in sterile conditions that is caused by inappropriate activation of the innate immune system [4,5]. Stigmata that are classically found in autoimmune diseases, such as high-titer autoantibodies and antigen-specific T lymphocyte activation, do not participate in the onset or continuation of AID inflammation [6]. Mutations in over 50 different genes have been reported to underlie AID [7], while a substantial proportion of patients suffer from non-Mendelian AID, such as periodic fever with aphthous stomatitis, pharyngitis and adenitis (PFAPA) syndrome, systemic-onset juvenile idiopathic arthritis (sJIA, pediatric Still's disease), or adult-onset Still's disease (AOSD) [8,9]. In contrast to AID, dysregulated lymphocyte activation and autoantibody formation are hallmark features of **autoimmune diseases (AI)** [10]. In AI, healthy tissues or cells are mistakenly targeted by the body's own immune system, which can lead to dysfunction or damage to specific organs and/or manifest with systemic inflammatory features, such as systemic lupus erythematosus (SLE), dermatomyositis (DM) and rheumatoid arthritis [11,12]. **Hyperinflammation (HI)** is a third subset of systemic inflammatory diseases that typically present as acute and potentially life-threatening. HI has been categorized as a subset of AID mainly because it is propagated by innate immune cell activation [13]. However, the pathogenesis of HI is often more intricate,

including impaired cell death by cytotoxic cells [14] and/or unhalted phagocytosis of hematopoietic cells [15]. Primary and secondary immunopathologies are found in HI, respectively known as hemophagocytic lymphohistiocytosis (HLH) or macrophage activation syndrome (MAS) [13]. In some patients presenting with HI, microbial infections may be the initial trigger, as has been observed during the coronavirus 2019 (COVID-19) pandemic in the majority of severe acute respiratory syndrome coronavirus 2 (SARS-CoV-2) infected patients in intensive care units [16].

As systemic inflammation is a common feature of these diseases, patients with AID, AI, or HI may present similarly. Despite clinical overlap, the underlying pathophysiology and subsequent patient management differ, making it challenging to diagnose and treat individuals. Many routine laboratory tests are abnormal in most patients, both during and between symptomatic episodes (e.g., increase in white blood cells (WBC), C-reactive protein (CRP), or erythrocyte sedimentation rate (ESR)). These parameters are non-specific and generally do not distinguish between different sources of inflammation.

Cytokines are small protein molecules (<40 kDa) produced and secreted by most human cells, acting as highly inducible and versatile immune signaling molecules [17].In recent years, studies on cytokines have increased our understanding of inflammation while simultaneously revealing its complexity [17,18]. Despite the complex architecture and dynamic cascade of events that precede and ensue the onset of systemic inflammation, multiple mediators can be delineated as disease-, context-, and patient-specific, which contrasts with clinically overlapping features [19]. As such, the evaluation of patients' individual cytokine profiles has emerged as a simple, relatively quick, cheap, and highly effective approach to guide diagnostic, prognostic, and therapeutic decision-making in human diseases, especially immune-related disorders [17,20,21].

In this study, we aimed to identify sensitive and specific serum cytokine signatures for three disease categories of systemic inflammatory disease (AID, systemic AI, and HI). For this, we performed machine learning and unbiased variable selection methods on serum concentrations of 55 inflammatory cytokines as measured by Meso Scale Discovery (MSD) in a cohort of 44 patients, grouped into three disease categories and collectively exhibiting more than 12 different well-defined inflammatory diseases. To facilitate future studies to validate group-specific cytokine signatures, we favored maximal accuracy with the smallest possible number of biomarkers. This led to the identification of a 5-plex cytokine panel that showed a unique and differentiating signature between disease categories.

Results

Cohort characteristics

We included 44 patients with active systemic inflammation (4 infants, 37 children, and 3 adults; overall median age 6.5y, [interquartile range (IQR) 3.8-13.3]) and 16 age-matched healthy individuals (**Table 1, Figure 1A-C**). Only samples from patients with known inflammatory diseases obtained during active (febrile) disease flares were included, excluding partial or complete remission status from the analyses. Among patients, 27 had active AID (including four patients with monogenic AID [*MEFV*, *NLRP3*, and *NOD2* variants], 13 sJIA/AOSD cases, and nine PFAPA patients), eight presented systemic AI (two SLE, three juvenile DM, and three scleroderma), nine showed HI (four with HLH in the first months of life [two with inborn errors in *PRF1* and *UNC13D*], and five patients with MAS, of which four patients had underlying sJIA or AOSD). Twenty-six patients were female (M/F ratio 1:1.4). Patients with systemic AI were exclusively female, as opposed to other subgroups with a balanced sex ratio (**Figure 1C**). The majority of patients had elevated white blood cell (WBC) count, absolute neutrophil count (ANC), C-reactive protein (CRP), erythrocyte sedimentation rate (ESR), and ferritin (**Figure 1D-H**). Patients with AID presented with higher WBC counts (11500/µl, [8610, 16340]), ANC (7390/µl, [5452, 10620]), and CRP (88.4 mg/l, [42.7, 175.8]). The highest ferritin levels were noted in patients with HI (12241 µg/l, [2468, 21425]). In the same group systemic steroids (55.6%) and biopharmaceuticals (22.2%) were most frequently used at the time of sampling. When multiple samples were available from the same patient, we used serum obtained when the patient was treatment-naive and/or at maximal inflammation (according to clinical assessment and routine laboratory parameters). Detailed patient characteristics and routine laboratory data are presented in supplementary data (**Table S1**).

Cytokine quantification

Fifty-five inflammatory cytokines were quantified in patients and controls (**Table S2**). Because of sample availability, two patients (an 11-year-old girl with MAS and a 3-year-old boy with PFAPA) had missing data for >20% of the cytokines and were excluded from further data analysis. Three cytokines (IL-21, IL-23, and IL-31) were excluded because of low detectability among patients and controls (i.e., IL-21, IL-23 and IL-31 respectively with 100%, 97.5% and 98.8% of data points below the lower detection limit). Because strong positive correlations were found between SAA and CRP (rho 0.87; P=3.43e-17), IL-6 and CRP (rho 0.80, P=3.95e-9), CXCL9 and IL-10 (rho 0.76, P=7.41e-13), CRP and CXCL9 were excluded from further analyses to prevent collinearity (**Figure 1I, Figure S1A-D**).

The remaining missing data (n=14/3016; 0.46%) were imputed using iterative PCA if a complete dataset was required for statistical analyses (e.g., PCA and regression models). All cytokine data were normalized for participants' ages using the median of age-matched healthy individuals. Through dimensionality reduction, we verified that adequate normalization by age group was present (**Figure S1E-G**). After these data cleaning steps, substantial overlap of patient groups was present when exploiting all remaining variables in a PCA with variance explaining up to 37.5% in the first two dimensions (**Fig. 1J**).

Cytokine profiles by disease group

Of the remaining 50 proteins included in the analysis, 36 (72%) were significantly upregulated or downregulated when comparing each disease group with healthy individuals (n=17 for systemic AI, n=23 for AID, and n=27 for HI) or across disease groups (n=18) (**Fig. 2A-B**). Levels of SAA, CXCL10, IL-6, IL-15, IFN-γ, and IL-10 levels were significantly altered in both comparisons (**Fig. S2A**). Most cytokines were either elevated (e.g., IL-1β, IL-3, and IL-6) or decreased (e.g., IL-17B, CCL17, and FGF2) when comparing distinct disease groups with HCs. Of the 18 cytokines with significant differences across disease groups, eight (IL-27, SAA,

ICAM-1, CCL26, IL-17A/F, Tie-2, IL-17C, and VCAM-1) showed incongruity between disease groups (e.g., reduced SAA in systemic AI but increased in AID and HI). CCL11, CCL13, CCL17, CXCL8, IL-3, IL-5, IL-7, IL-12/IL-23p40, IL-12p70, IL-17A, MIP-1α, TNF, VEGF-A, and VEGFR-1 were excluded from model building because their levels did not differ among disease groups or between any of the disease groups and HCs (**Fig. S2A-B**).

Unsupervised hierarchical clustering of normalized patient data showed substantial heterogeneity of the 36 proteins between individual patients and the three patient groups (Fig. 2C). Patients with systemic AI clustered together, suggesting a relative closeness in their cytokine profiles. Other patient groups and their routinely assessed inflammatory markers were dispersed, along with dissimilar levels of multiple cytokines. To varying degrees, multiple cytokines positively correlated with routine laboratory markers (**Fig. S2C**). After correcting for multiple testing, correlations with the highest statistical significance were found between IL-6 and CRP (P=1.9e-4), IL-6 and ESR (P=5.3e-4), and IL-1Ra and ANC (P=1.5e-3), and all of which have been previously reported to correlate [22–25] confirming the biological relevance of our assay (**Fig. S2D-F**).

Machine learning

The 36 proteins with significant differences between disease groups and/or between disease groups and HCs served as inputs (predictor variables) for three regression models. In these models, the diagnostic groups (HI, AID, and systemic AI) functioned as the outcome variables. On the patients' normalized dataset, we performed repeated runs (n=1000) of 1) random forest regression, whereby variable importance was defined as the mean decrease in Gini Impurity (**Fig. 3A**); and 2) Multivariate methods with Unbiased Variable Selection in R (MUVR), in which we retained the maximum number of optimal variables (**Fig. 3B**); and 3) Boruta, which is a wrapper algorithm for random forests that selects all the relevant features (**Fig. 3C**). Using

these three approaches, highly similar protein sets were retained with prioritization of SAA, ICAM-1, and CXCL10 (**Fig. 3D**). All variables identified as relevant by MUVR (n=8) were among the most important variables retained by random forest regression and Boruta (**Fig. 3E**). IL-1β was the only protein ranked as relevant by Boruta, whereas it was not deemed important by the other algorithms (Fig. 3F). The common cytokines among the three algorithms were CCL26, CXCL10, ICAM-1, IL-10, IL-17C, IL-27, SAA, and Tie-2 (**Fig. 3F**).

As a sensitivity analysis, we applied the same three regression models (1000 repeats of each algorithm) on the patients' normalized dataset, but iteratively excluded one disease group (HI, AID, or systemic AI consecutively) (**Fig. S3A-I**). Consistent with the analyses performed on the full dataset, MUVR was most selective. Except for CCL22 and IL-16 (selected in the analysis without systemic AI) (**Fig. S3G-I**), MUVR only identified cytokines that were equally retained by the other algorithms in every comparison. Sensitivity analyses further revealed that the relative importance of some biomarkers was significantly influenced by the composition of the patient cohort. Examples include Tie-2 and MIP-3α, both of which show heightened importance when analyzing data without HI (**Fig. S3B**) and AID (**Fig. S3E**), respectively. SAA was not withheld without systemic AI (**Fig. S3H-I**), whereas it was ranked first in the other scenarios (**Fig. S3B, Fig. S3E**).

Selection of cytokines with highest importance

When aggregating the data of the original and sensitivity analyses, no common cytokines were found (i.e., none were retained by each algorithm and with each comparison) (**Fig. 4A**). To identify the most robust set of cytokines, we mined all machine learning data and aimed to 1) select highly specific biomarkers, and 2) prioritize those with consistent importance across algorithms. To rationalize this process and to select robust variables, we first selected cytokines that were retained in the original analysis and by at least two out of three comparisons in the

sensitivity analyses. This allowed for the inclusion of CXCL10 and SAA, which were deemed important by all algorithms, except for the sensitivity analyses without AID and AI, respectively (**Fig. 4A**). Next, we sorted the cytokines based on variable importance, considering the median of metrics as determined by the different algorithms (**Fig. 4B**). In addition to CXCL10 and SAA, and using the summed ranks as an overall importance indicator, we identified superior performance of IL-27, ICAM-1, and CCL26. In contrast to SAA and CXCL10, these three additional biomarkers showed consistent performance across all sensitivity analyses and were preferentially selected using all three regression methods (**Fig. S4A-B**). The mean ranking of the top five cytokines was equal to or less than 8.4, indicating that these cytokines, on average, were ranked in the first quartile across all analyses and using all three regression models (**Fig. S4C**).

Logistic regression modelling

Using the five prioritized cytokines (CCL26, CXCL10, ICAM-1, IL-27, and SAA) as predictor variables, binomial logistic regression modelling allowed for the characterization of a statistically significant signature for each patient group (P-values of 1.34e-4, 2.20e-7, and 2.21e-7, and pseudo-R^2 values of 0.56, 0.66, and 0.89 for HI, AID, and AI, respectively) (**Fig. 4C**). Analyzing cytokines individually, we found that patients with high ICAM-1 levels showed a significantly increased risk (adjusted odds ratio) of HI (P=0.028). Although patients with HI showed clearly elevated SAA levels compared to healthy controls, the relative amount of SAA as opposed to patients with other types of systemic inflammation was decreased (P=0.048). This feature contrasts with patients with AID, who showed a trend for lower ICAM-1 (P=0.091), and reduced CXCL10 (P=0.032) levels, but an elevated odds ratio for SAA (P=0.003). Patients with systemic AI showed significantly reduced odds ratios for SAA (P=0.014) and a trend for higher CXCL10 levels (P=0.118). A direct comparison of the normalized data in our patients confirmed significantly lower IL-27 and CCL26 in systemic AI

compared to AID, and even higher values in HI. We found low CXCL10 in AID compared to both HI and systemic AI and high ICAM-1 in HI compared to AID and AI. The highest SAA was found in AID (**Fig. S4D**). Besides that SAA correlated positively with CRP, none of the five cytokines showed a strong correlation with routine laboratory tests, indicating that this selection method has the potential to add more specificity to clinical data (**Fig. S4E**).

Performance of the models and included cytokines

By iterative calculation of the area under the curve (AUC) for each model, we confirmed that the statistical significance of the models was associated with excellent predictive power for AID (mean AUC 0.91) and systemic AI (0.94), and good performance for HI (0.81) (**Fig. 4D**). To corroborate these findings, we used the five prioritized variables as inputs for unsupervised hierarchical clustering and PCA. Performing k-means partitioning on hierarchically clustered data revealed an adequate separation of patient groups (Fig. 4E). In addition, PCA with the five prioritized cytokines separated the majority of the patients into three distinct clusters corresponding to their known diagnosis (**Fig. 4F**).

We verified our selection by assessing the degree of statistical significance of the 5-plex panel in comparison with more restrictive and extensive selections of cytokines (using the order of cytokines by their sum of ranks to add or exclude cytokines) (**Fig. S4F**). This analysis confirmed that the 5-plex assay showed a higher statistical significance ($P<0.001$) than smaller sets of cytokines, particularly because of better performance of the HI signature. Adding more biomarkers as predictor variables allowed for small improvements in the P-value only for HI, but less significance (and thus increased inaccuracy) was found for AID and systemic AI (**Fig. S4G**). We concluded that the five prioritized cytokines were the most favorable selection because they exhibited excellent statistical significance and are good candidates for future validation studies on larger cohorts owing to their narrow selection.

Finally, to explore possible overfitting of our models, we verified the degree of multicollinearity in the 5-plex panel. First, we assessed the Spearman correlation coefficients between each variable pair, verifying that none of the cytokines showed consistent positive or negative correlations in each patient group (**Fig. S4H**). Second, for each cytokine in each model, we estimated the variance inflation factor (VIF), where a VIF >10 was considered unacceptable. We established a maximum VIF of 6.071 in our analysis (ICAM-1 in the HI model). Despite these results, the statistical significance of our selection in each binomial model could not be confirmed by multinomial logistic regression (data not shown). Given that we corrected for highly correlated proteins prior to unbiased variable selection (excluding CXCL9 and CRP), and that our review for multicollinearity was favorable, we presume that the relatively small sample size of our cohort may be accounted for [26]. Future research in larger patient cohorts should thus allow the verification of the statistical significance of our panel using multinomial regression models.

Discussion

From a clinical perspective, the diagnosis and treatment of patients with systemic inflammatory diseases is challenging. Its broad and age-dependent differential diagnosis and non-specificity of clinical symptoms and routine laboratory abnormalities frequently lead to delays or misclassifications in diagnosis, contributing to additional morbidity and mortality [27]. Distinguishing between different sources of systemic inflammation is important, as they require different approaches in further diagnostics and, if falsely indicated, may lead to opposing and potentially harmful treatments (e.g., corticosteroids in infection). Performing an efficient and relevant work-up for patients with suspected systemic inflammation is thus of pivotal importance in order to avoid patients visiting multiple clinicians, having various (mis)diagnoses, undergoing unnecessary tests and incorrect treatments and increased medical expenses [28,29]. In addition to disease awareness and paucity of clinical criteria, an important determinant of the challenges in these patient groups is the lack of robust functional tests [30].

Confronted with the challenges encountered in daily clinical practice, we established a cohort of 44 patients with various systemic inflammatory diseases and analyzed 55 inflammatory cytokines in their blood samples. From this, we proposed a panel of five cytokines that we identified using three unbiased machine learning methods, that showed robust performance in logistic regression modelling and dissected patient groups by unsupervised hierarchical clustering and dimensionality reduction algorithms.

Our 5-plex panel comprises a unique combination of proteins. Nevertheless, previous studies have linked these five cytokines to multiple inflammatory pathways and/or human diseases. Serum amyloid A (**SAA**) is the most well-studied protein of the selection. SAA is a nonspecific acute-phase protein predominantly synthesized in the liver. For more than 40 years, SAA has an unwavering presence in medical literature because of its association with amyloidosis

[31,32]. A large and ever-growing body of literature has linked elevated SAA levels to a plethora of autoimmune and autoinflammatory diseases, as extensively reviewed recently [33]. Interestingly, in AID populations, SAA was found to not always correlate directly with elevated CRP levels [34–36]. In our cohort, the highest SAA level was found in patients with AID, making it an independent predictor of AID (and it related to significantly low odds for HI or systemic AI). It should be noted that patients with HI also showed a clear SAA elevation, but the relative increase was lower, which might be related to higher proportion of patients on corticosteroids in this group. In systemic AI, low SAA could be correlated with the absence of a clear acute phase response, whereas routine laboratory tests did not suggest a similar association in HI.

CCL26 is primarily secreted by non-hematopoietic cells and is chemotactic to eosinophils. It is a prototypical Th2 related cytokine with well-described roles in eosinophilic oesophagitis [37] and asthma [38]. In this context, the CCR3 agonist effects of CCL26 have been best studied, but its antagonistic effects on CCR1, CCR2, and CCR5 have led to the hypothesis that CCL26 may have broader and immunomodulatory roles [39]. More recent research has experimentally confirmed that CCL26 has chemorepulsive properties on monocytes [40] and CCL26 has been found to be elevated in COVID-19, including an association with severity [41,42]. Thus, it may be no surprise that the highest CCL26 level in our cohort was found in patients with HI.

The intercellular adhesion molecule (**ICAM**)**-1** is an extensively studied transmembrane glycoprotein of the immunoglobulin superfamily. As an adhesion molecule typically expressed on the vascular endothelium, ICAM-1 plays a prominent role in cell trafficking [43]; however, additional roles in the onset and resolution of inflammation, immune cell effector functions, and tumorigenesis have recently emerged [44]. In line with our cohort, where elevated ICAM-1 is a predictor of HI, experimental evidence points towards ICAM-1 being a macrophage

activation marker [45,46] and having a non-redundant role in macrophage efferocytosis [47]. Correspondingly, soluble ICAM-1 levels were drastically elevated in patients with systemic inflammatory response syndrome [48].

Most of our patients showed elevated **IL-27** levels compared to healthy controls, which is in line with the diverse roles that IL-27 plays in innate and adaptive immune responses [49,50]. As an IL-12 cytokine family member produced by antigen-presenting cells upon Toll-like receptor binding, it is not surprising that IL-27 has been described as a biomarker for bacterial infection [51,52]. IL-27 has a dominant role in Th1 differentiation. However, immune regulatory properties (induction of Th17 cells and IL-10) have also been associated with IL-27 [49]. Hence, interest in IL-27 has increased in the context of AI [53,54]. In our cohort, not all patients with systemic AI presented with elevated IL-27 levels, although elevated levels in HI might be related to the high degree of immune dysregulation and Th1 skewing in these patients.

CXCL10 is another molecule functionally categorized as a Th1 cytokine. CXCL10, also known as IFN-γ-induced protein 10 (IP-10), is a chemokine downstream of type I and type II interferon signaling that regulates chemotaxis of CXCR3+ immune cells [55–57]. It has pleiotropic effects and is associated with infectious [58] and autoimmune disease [59]. It is expected that CXCL10 is significantly elevated in our patients compared to HCs, although heterogeneity exists between disease groups. Compared to other patients, we had arguments for less prominent inflammation in our patients with systemic AI (who showed low CRP and relatively low levels of most prioritized cytokines). However, this finding was in sharp contrast to CXCL10 levels. CXCL10 was clearly increased in patients with systemic AI compared to patients with AID and HCs and exhibited a trend for elevated odds of systemic AI.

It is noteworthy that certain 'classical' cytokines, such as IFNγ and IL-18, commonly associated with hyperinflammation, were not prioritized by our methods. While this may seem unexpected,

we propose that it reflects the strength of our unbiased approach. The absence of these cytokines in our selection does not imply they lack relevance in the pathophysiology of specific inflammatory conditions; rather, it indicates that they are less effective in distinguishing between the disease states examined in this study.This study has several limitations. First, data were generated from a stringent selection of patients with active disease, and blood samples were obtained only from treatment-naïve patients and/or those with maximal clinical inflammation. In daily practice, inflammatory cytokine profiles may be pharmacologically altered or under the dynamic influence of the natural disease course, potentially leading to variations in their blood protein levels. Second, we attempted to include a broad spectrum of inflammatory diseases; however, our cohort did not include the full clinical heterogeneity of the three disease groups. Additional nuances in cytokine signatures could be present between or within the disease groups, which we could not probe in sufficient detail because of our sample size. Similarly, the input variables (selection of assays) may have been subject to a selection bias. We included the broadest possible assay list for the technology that we used; however, given that these are commercially available and preconfigured kits, they may have been selected for specific characteristics outside the scope of scientific research. Evidently, our analyses reveal associative data, whereby altered presence of cytokines in the systemic circulation could be causative but could also represent secondary host responses to active disease. Cytokines found to be highly accurate in our regression models may be nonspecific or insensitive to other patients in alternative clinical settings. Finally, we excluded cytokines with a large majority of data points below the limit of detection. The low sensitivity of certain biomarkers does not exclude the possibility that they can be biologically relevant in subdetectable concentrations and/or in compartments other than the systemic circulation. Further research is needed to investigate the relevance of cytokine measurements to distinguish among other inflammatory states, such as infection and/or malignancy.

In conclusion, based on a representative cohort of patients, we delineated a 5-plex cytokine panel that could differentiate between patients with HI, AID, and systemic AI. Our unique signature consisted of CCL26, CXCL10, ICAM-1, IL-27, and SAA, all of which play diverse roles in inflammatory pathways and human diseases. We propose that future studies include prospective validation of this 5-plex cytokine panel in larger groups to provide answers to the remaining questions and address the specificity and sensitivity of the proposed selection. These results will contribute to a better understanding of the pathophysiology and improve early diagnosis and management of patients with systemic inflammation.

Methods

Selection of patients and controls

Pediatric and adult patients with known systemic inflammatory diseases were included in this study. Patient diagnoses were confirmed by medical experts and based on universal clinical criteria and/or genetic investigations. Age-matched individuals volunteered to serve as healthy controls (HCs). HCs denied prior medical history and had no infection or vaccination at the time of sampling or in the previous six weeks. The biological sex and age of all the participants were recorded. Because we used matched HCs, sex was not considered as a biological variable. We documented the confirmed diagnosis (including genetic results), current clinical status (symptoms of ongoing inflammation), and current medications (with or without an immunomodulatory effect). Patients could not participate if probable or confirmed infections contributed to disease activity.

Patients, HCs, and/or their legal representatives provided written informed consent for study participation, in accordance with the 1975 Declaration of Helsinki. Ethical approval for collection, biobank storage, and analysis of data and materials from patients and healthy individuals was granted by the main Ethical Committee of the Ghent University Hospital (BB190105), as well as by local committees of participating centers. The demographic and clinical data of the participants were registered in an in-house stored, protected, and anonymized data file.

Blood sampling

Venous blood was collected from patients and HCs in serum tubes. Within 60 min of sampling, clotted blood tubes were spun at 4°C, and cell-free serum was aliquoted and stored in a temperature-monitored freezer at −80°C until analysis. When multiple samples were available from the same patient, we used serum obtained when the patient was treatment-naive and/or at

maximal inflammation (according to clinical assessment and routine laboratory parameters). Only samples from patients with known inflammatory diseases obtained during active disease flares were included, excluding partial or complete remission status from the analyses. In some patients, retrospective samples were retrieved from our biobank after confirmation of a specific diagnosis. The oldest included sample was dated January 3th, 2017 (2052 days of storage). The median age of sample storage was 201 days, and 85% of the included samples were stored for less than 1000 days.

Cytokine quantification

Cytokines were quantified in freshly thawed sera using electrochemiluminescence technology with Meso Scale Discovery (MSD; Meso Scale Diagnostics, Rockville, Maryland, USA). All consumables, antibody sets, and multiarray plates were used as provided in the MSD assay kits. We used seven different human V-plex kits, including the Proinflammatory Panel 1 (K15049D; measuring IFN-γ, IL-1β, IL-2, IL-4, IL-6, IL-8, IL-10, IL-12p70, IL-13, and TNF), Cytokine Panel 1 (K15050D; GM-CSF, IL-1α, IL-5, IL-7, IL-12/IL-23p40, IL-15, IL-16, IL-17A, TNF-β, and VEGF-A), Cytokine Panel 2 (K15084D; IL-1RA, IL-3, IL-9, IL-17A/F, IL-17B, IL-17C, IL-17D, and TSLP), Chemokine Panel 1 (K15047D; Eotaxin, Eotaxin-3, IL-8, IP-10, MCP-1, MCP-4, MDC, MIP-1α, MIP-1β, and TARC), TH17 Panel 1 (K15085D; IL-17A, IL-21, IL-22, IL-23, IL-27, IL-31, and MIP-3α), Angiogenesis Panel 1 (K15190D; FGF (basic), PlGF, Tie-2, VEGF-A, VEGF-C, VEGF-D, and VEGFR-1/Flt-1), and Vascular Injury Panel 2 (K15198D; CRP, ICAM-1, SAA, and VCAM-1) kits. IL-18 and MIG levels were quantified using separate antibody sets (B21VJ and F210I, respectively) and a 2-SECTOR U-plex Development Pack (K15227N). The assays were performed according to the manufacturer's instructions. Sera was diluted as proposed by the manufacturer, being 1:2 for analytes measured in Proinflammatory Panel 1, Cytokine Panel 1 and Angiogenesis Panel 1 kits, 1:4 for the Chemokine panel 1, Cytokine panel 2, Th17 panel and the U-plex (IL-18 and MIG) kits, and 1:1000 for the Vascular

injury Panel 2 kit. Phosphate-buffered saline (PBS; 14190250, Gibco) supplemented with 0.05% Tween (P1379, Sigma-Aldrich) was used as wash buffer. Plates were read in MSD Gold Buffer on a MESO QuickPlex SQ 120MM using the Methodical Mind software (Meso Scale Diagnostics).

Data cleaning and normalization

For each cytokine, the background signal was defined as the sum of the mean and 2 × the standard deviation of the signal of two blank wells on each plate. This background signal was subtracted from the raw data for each cytokine, whereby a value of 1 was imputed for negative values to allow for normalization in subsequent steps. Cytokines with less than 20% of samples within the range defined by the lower (background signal) and upper detection limits (mean of the highest calibrator) were excluded from the dataset. Patients with more than 20% missing data (due to insufficient sample volume) were excluded from further analysis. For biomarkers that were measured in duplicate on different plates (i.e., IL-17A, VEGF-A and IL-8), one of both measurements was omitted based on the comparison of i) the number of samples within range of the calibrator (for IL-8 100% samples were within range at 1:2 dilution in 'Proinflammatory panel 1' as opposed to 83.5% were within range at 1:4 in 'Chemokine panel 1') or ii) the number of missing values (for VEGF-A n=1 missing in 'Cytokine panel 1' as opposed to n=4 missing in 'Angiogenesis panel 1', and for IL-17A none were missing in 'Th17 panel 1' as opposed to n=1 missing in 'Cytokine panel 1'). Before excluding these values, we verified that duplicate measurements were strongly correlated with one another (i.e., IL-8: Spearman rho 0,3482 (P=0,0019); VEGF-A: rho 0,9905 (P<0.0001); and IL-17A: rho 0,6264 (P<0.0001)). For analyses requiring a complete dataset (such as principal component analysis (PCA) and regression models), missing values were imputed by an iterative PCA model using the CRAN package *missMDA* (v1.18). Prior to regression analyses, collinearity between predictor variables was verified using Spearman correlation test and calculation of Benjamini-

Hochberg adjusted p-values. Pairs of biomarkers from patients and HCs with a Spearman rho >= 0.75 and an adjusted p-value <0.05 were considered to correlate strongly and to be ineligible for independent prediction of the outcome value. To compare data across age groups, the log2 fold change over the median of age-matched HCs (infants (<1yo), children (1-18yo) and adults (>18yo) separately) was calculated for each cytokine signal of each sample.

Machine learning analyses

Unbiased variable selection was performed by three different algorithms in R. Random forest (RF) regression was done using Breiman's random forest algorithm as available in the randomForest package (v4.7-1.1). For each iteration (n=1000), we grew 1000 trees with seven variables randomly sampled as candidates at each split. Twenty-two samples (63.25 %) were collected for each disease group. Variable importance was defined as the decrease in Gini index averaged over all trees. The top half of the variables, sorted based on the decrease in Gini index, were deemed important. Second, we used Multivariate methods with Unbiased Variable Selection in R (MUVR, v0.0.975) as described by Shi et al.[60]. For each MUVR, we performed 1000 repetitions and used random forests as the core modelling algorithm, defining eight outer cross-validation segments (the maximum of the smallest group), including 75% of the variables per iteration. Variables were ranked on variable importance of projection (VIP) (median for 1000 repetitions), where lower is better. The all-relevant model ("max" model) selected the number of variables. For the third algorithm, we used Boruta (*boruta* package v8.0.0), a wrapper method built around Random Forest Regression. The z-score of the Mean Decrease in Accuracy (default setting) was used as the performance metric, and a maximum of 1000 iterations was performed. Variables were selected as important with a median z-score higher than the maximum shadow attributes (permuted copies were random and shuffled copies of all features). To summarize the three machine learning methods we used the *scale* function

in R. As an overall importance metric, ranks were calculated for each cytokine based on the median value of the corresponding metric in each algorithm and dataset.

Logistic regression modelling

Binomial logistic regression was performed on the normalized cytokine data with the *glm* function of the base *stats* package in R. The variables of patients in one disease group were compared with those of all other patients. Odds ratios were calculated as exponentiates of the coefficient estimates. The lower and upper bounds of the 95% confidence intervals were calculated using *qnorm* and the coefficient standard error. The significance of each model compared to a null modell (y~1) was calculated using chi-square. The McFadden Pseudo-R^2 and variance inflation factor (VIF) were retrieved for each model using *jtools*. Multinomial logistic regression analysis was performed using the *nnet* package.

The area under the curve (AUC) was calculated on thousand iterations of random splitting the patient data in a training (75%) and test (25%) set (with verification that each set contained at least one patient of each disease group), performing quasibinomial logistic regression on the training set and calculating the AUC on the predicted outcome of the test set using the *ROCR* package.

General statistics and data analysis

All tests were two-sided and Benjamini-Hochberg corrections were applied for multiple testing when indicated. The specific statistical methods are described in the figure legends. Results with a P-value of less than 0.05 were considered significant. Significance levels were and denoted as *, $P < 0.05$; **, $P < 0.01$; ***, $P < 0.001$; and ****, $P < 0.0001$. All data analysis was performed in RStudio v2022.07.2 (R version 4.2.2). The following CRAN packages were used: *caTools* (v1.18.2), *Boruta* (v8.0.0), *broom* (v1.0.3), *caret* (v6.0-93), *circlize* (v0.4.15),

ComplexHeatmap (v2.12.1), *corrplot* (v0.92), *cowplot* (v1.1.1), *doParallel* (v1.0.17), *dplyr* (v1.0.10), *factoextra* (v1.0.7), *fastDummies* (v1.6.3), *flextable* (v0.9.1), *forcats* (v1.0.0), *forestmangr* (v0.9.4), *ggbreak* (v0.1.1), *ggforce* (v0.4.1), *ggplot2* (v3.4.1), *ggpubr* (v0.6.0), *ggsignif* (v.0.6.4), *ggvenn* (v0.1.9), *gridExtra* (v2.3), *Hmisc* (v4.8-0), *jtools* (v2.2.1), *magrittr* (v2.0.3), *MASS* (v7.3-58.1), *missMDA* (v1.18), *MUVR* (v0.0.975), *nnet* (v7.3.18), *plyr* (v1.8.8), *randomForest* (v4.7-1.1), *RColorBrewer* (v1.1-3), *remotes* (v2.4.2), *reshape* (v0.8.9), *ROCR* (v1.0-1), *rstatix* (v0.7.2), *smplot2* (v0.1.0), *stats* (v3.6.2), *tableone* (v0.13.2), *tibble* (v3.1.8), *tidyr* (v1.3.0), *tidyverse* (v2.0.0)

Data availability

Normalized cytokine and clinical data of individual patients is available in Supplementary Materials.

Author contributions

Levi Hoste (LH) and Filomeen Haerynck (FH) conceptualized the study. LH and FH drafted the study protocol. LH analyzed and interpreted the data. Benson Ogunjimi, Rik Joos, Vito Sabato, Khadija Guerti, Jeroen van der Hilst, Jeroen Bogie, Peggy Jacques, Steven Callens, Joke Dehoorne and FH included patients and/or had roles in methodology supervision, data analysis and interpretation. Karlien Claes aided in patient-oriented care. Veronique Debacker performed experiments. Fleur Janssen performed experiments and collected clinical data. FH provided funding. LH drafted the initial version of the manuscript.

Acknowledgments

This research was conducted in the absence of any commercial or financial relationships that could be construed as potential conflicts of interest.

This project is funded by the Fonds voor Wetenschappelijk Onderzoek (FWO) under the program for Applied Biomedical Research with a Primary Social finality (TBM) (T004721N). LH also received funding from the Grand Challenges Programs of the Vlaams Instituut voor Biotechnologie (VIB). FH is supported by Ghent University research grant (BOF-UGent), Grand Challenges Programs of VIB and Jeffrey Modell Foundation. ST is beneficiary of a postdoctoral FWO grant. BO received funding from the FWO as senior clinical investigator (1861219N).

We wish to thank all patients, family members, healthy individuals, and staff from all the units that participated in the study.

References

1. Medzhitov R. Inflammation 2010: new adventures of an old flame. Cell. 2010;140:771–6.

2. Medzhitov R. The spectrum of inflammatory responses. Science (1979) [Internet]. 2021 [cited 2023 Feb 20];374:1070–5. Available from: https://www.science.org/doi/10.1126/science.abi5200

3. Medzhitov R. Origin and physiological roles of inflammation. Nature [Internet]. 2008 [cited 2023 Feb 20];454:428–35. Available from: https://www.nature.com/articles/nature07201

4. Dinarello CA. IL-1: discoveries, controversies and future directions. Eur J Immunol. 2010;40:599–606.

5. de Jesus AA, Canna SW, Liu Y, Goldbach-Mansky R. Molecular mechanisms in genetically defined autoinflammatory diseases: disorders of amplified danger signaling. Annu Rev Immunol. 2015;33:823–74.

6. Kastner DL, Aksentijevich I, Goldbach-Mansky R. Autoinflammatory Disease Reloaded: A Clinical Perspective. Cell [Internet]. 2010;140:784–90. Available from: https://doi.org/10.1016/j.cell.2010.03.002

7. Tangye SG, Al-Herz W, Bousfiha A, Cunningham-Rundles C, Franco JL, Holland SM, et al. Human Inborn Errors of Immunity: 2022 Update on the Classification from the International

553 Union of Immunological Societies Expert Committee. J Clin Immunol [Internet].
554 2022;42:1473–507. Available from: https://doi.org/10.1007/s10875-022-01289-3

555 8. Nigrovic PA, Lee PY, Hoffman HM. Monogenic autoinflammatory disorders: Conceptual
556 overview, phenotype, and clinical approach. Journal of Allergy and Clinical Immunology
557 [Internet]. 2020;146:925–37. Available from: https://doi.org/10.1016/j.jaci.2020.08.017

558 9. Touitou I. Inheritance of autoinflammatory diseases: Shifting paradigms and nomenclature.
559 J Med Genet. 2013;50:349–59.

560 10. Doria A, Zen M, Bettio S, Gatto M, Bassi N, Nalotto L, et al. Autoinflammation and
561 autoimmunity: Bridging the divide. Autoimmun Rev [Internet]. 2012;12:22–30. Available
562 from: https://www.sciencedirect.com/science/article/pii/S1568997212001541

563 11. Cooper GS, Stroehla BC. The epidemiology of autoimmune diseases. Autoimmun Rev
564 [Internet]. 2003;2:119–25. Available from:
565 https://www.sciencedirect.com/science/article/pii/S1568997203000065

566 12. Davidson A, Diamond B. Autoimmune Diseases. New England Journal of Medicine
567 [Internet]. 2001;345:340–50. Available from: https://doi.org/10.1056/NEJM200108023450506

568 13. Schulert GS, Canna SW. Convergent pathways of the hyperferritinemic syndromes. Int
569 Immunol. 2018;30:195–203.

570 14. Pachlopnik Schmid J, Côte M, Ménager MM, Burgess A, Nehme N, Ménasché G, et al.
571 Inherited defects in lymphocyte cytotoxic activity. Immunol Rev. 2010;235:10–23.

572 15. de Saint Basile G, Ménasché G, Latour S. Inherited defects causing hemophagocytic
573 lymphohistiocytic syndrome. Ann N Y Acad Sci. 2011;1246:64–76.

574 16. Mehta P, McAuley DF, Brown M, Sanchez E, Tattersall RS, Manson JJ, et al. COVID-19:
575 consider cytokine storm syndromes and immunosuppression. The Lancet [Internet].
576 2020;395:1033–4. Available from: http://dx.doi.org/10.1016/S0140-6736(20)30628-0

577 17. Dinarello CA. Historical insights into cytokines. Eur J Immunol [Internet]. 2007 [cited 2023
578 Feb 24];37:S34–45. Available from:
579 https://onlinelibrary.wiley.com/doi/full/10.1002/eji.200737772

18. Gabay C, Kushner I. Acute-phase proteins and other systemic responses to inflammation. N Engl J Med. 1999;340:448–54.

19. Schett G, McInnes IB, Neurath MF. Reframing Immune-Mediated Inflammatory Diseases through Signature Cytokine Hubs. New England Journal of Medicine [Internet]. 2021;385:628–39. Available from: https://doi.org/10.1056/NEJMra1909094

20. Chetaille Nézondet AL, Poubelle PE, Pelletier M. The evaluation of cytokines to help establish diagnosis and guide treatment of autoinflammatory and autoimmune diseases [Internet]. J Leukoc Biol. John Wiley and Sons Inc.; 2020 [cited 2020 Feb 28]. p. JLB.5MR0120-218RRR. Available from: https://onlinelibrary.wiley.com/doi/abs/10.1002/JLB.5MR0120-218RRR

21. Kopf M, Bachmann MF, Marsland BJ. Averting inflammation by targeting the cytokine environment. Nat Rev Drug Discov [Internet]. 2010;9:703–18. Available from: https://doi.org/10.1038/nrd2805

22. Heinrich PC, Castell J V, Andus T. Interleukin-6 and the acute phase response. Biochem J. 1990;265:621–36.

23. Slaats J, Ten Oever J, van de Veerdonk FL, Netea MG. IL-1β/IL-6/CRP and IL-18/ferritin: Distinct Inflammatory Programs in Infections. PLoS Pathog. 2016;12:e1005973.

24. McColl SR, Paquin R, Ménard C, Beaulieu AD. Human neutrophils produce high levels of the interleukin 1 receptor antagonist in response to granulocyte/macrophage colony-stimulating factor and tumor necrosis factor alpha. J Exp Med. 1992;176:593–8.

25. van Leeuwen MA, Westra J, Limburg PC, van Riel PL, van Rijswijk MH. Clinical significance of interleukin-6 measurement in early rheumatoid arthritis: relation with laboratory and clinical variables and radiological progression in a three year prospective study. Ann Rheum Dis. 1995;54:674–7.

26. Nemes S, Jonasson JM, Genell A, Steineck G. Bias in odds ratios by logistic regression modelling and sample size. BMC Med Res Methodol [Internet]. 2009;9:56. Available from: https://doi.org/10.1186/1471-2288-9-56

607 27. Kallinich T, Gattorno M, Grattan CE, De Koning HD, Traidl-Hoffmann C, Feist E, et al.
608 Unexplained recurrent fever: When is autoinflammation the explanation? Allergy: European
609 Journal of Allergy and Clinical Immunology [Internet]. 2013 [cited 2020 Feb 26];68:285–96.
610 Available from: http://www.ncbi.nlm.nih.gov/pubmed/23330689

611 28. Lachmann HJ. Periodic fever syndromes. Best Pract Res Clin Rheumatol. Bailliere Tindall
612 Ltd; 2017. p. 596–609.

613 29. Ozen S, Kuemmerle-Deschner JB, Cimaz R, Livneh A, Quartier P, Kone-Paut I, et al.
614 International Retrospective Chart Review of Treatment Patterns in Severe Familial
615 Mediterranean Fever, Tumor Necrosis Factor Receptor–Associated Periodic Syndrome, and
616 Mevalonate Kinase Deficiency/Hyperimmunoglobulinemia D Syndrome. Arthritis Care Res
617 (Hoboken) [Internet]. 2017 [cited 2020 Feb 26];69:578–86. Available from:
618 https://onlinelibrary.wiley.com/doi/abs/10.1002/acr.23120

619 30. Schnappauf O, Aksentijevich I. Current and future advances in genetic testing in systemic
620 autoinflammatory diseases. Rheumatology (Oxford). 2019;58:vi44–55.

621 31. Benson MD, Cohen AS. Serum amyloid A protein in amyloidosis, rheumatic, and neoplastic
622 diseases. Arthritis & Rheumatism: Official Journal of the American College of Rheumatology.
623 1979;22:36–42.

624 32. Meretoja J, Natvig JB, Husby G. Amyloid-related serum protein (SAA) in patients with
625 inherited amyloidosis and certain viral conditions. Scand J Immunol. 1976;5:169–74.

626 33. Sorić Hosman I, Kos I, Lamot L. Serum Amyloid A in Inflammatory Rheumatic Diseases:
627 A Compendious Review of a Renowned Biomarker. Front Immunol [Internet]. 2021;11.
628 Available from: https://www.frontiersin.org/articles/10.3389/fimmu.2020.631299

629 34. Yalçınkaya F, Çakar N, Acar B, Tutar E, Güriz H, Elhan AH, et al. The value of the levels
630 of acute phase reactants for the prediction of familial Mediterranean fever associated
631 amyloidosis: a case control study. Rheumatol Int [Internet]. 2007;27:517–22. Available from:
632 https://doi.org/10.1007/s00296-006-0265-6

633 35. Çakan M, Karadağ ŞG, Tanatar A, Sönmez HE, Ayaz NA. The Value of Serum Amyloid
634 A Levels in Familial Mediterranean Fever to Identify Occult Inflammation During
635 Asymptomatic Periods. JCR: Journal of Clinical Rheumatology [Internet]. 2021;27. Available

from:
https://journals.lww.com/jclinrheum/fulltext/2021/01000/the_value_of_serum_amyloid_a_levels_in_familial.1.aspx

36. Lofty HM, Marzouk H, Farag Y, Nabih M, Khalifa IAS, Mostafa N, et al. Serum Amyloid A Level in Egyptian Children with Familial Mediterranean Fever. Int J Rheumatol [Internet]. 2016;2016:7354018. Available from: https://doi.org/10.1155/2016/7354018

37. Blanchard C, Wang N, Stringer KF, Mishra A, Fulkerson PC, Abonia JP, et al. Eotaxin-3 and a uniquely conserved gene-expression profile in eosinophilic esophagitis. J Clin Invest. 2006;116:536–47.

38. Provost V, Larose M-C, Langlois A, Rola-Pleszczynski M, Flamand N, Laviolette M. CCL26/eotaxin-3 is more effective to induce the migration of eosinophils of asthmatics than CCL11/eotaxin-1 and CCL24/eotaxin-2. J Leukoc Biol. 2013;94:213–22.

39. Stubbs VEL, Power C, Patel KD. Regulation of eotaxin-3/CCL26 expression in human monocytic cells. Immunology [Internet]. 2010;130:74–82. Available from: https://doi.org/10.1111/j.1365-2567.2009.03214.x

40. Hummitzsch L, Berndt R, Kott M, Rusch R, Faendrich F, Gruenewald M, et al. Hypoxia directed migration of human naïve monocytes is associated with an attenuation of cytokine release: indications for a key role of CCL26. J Transl Med [Internet]. 2020;18:404. Available from: https://doi.org/10.1186/s12967-020-02567-7

41. Abers MS, Delmonte OM, Ricotta EE, Fintzi J, Fink DL, de Jesus AAA, et al. An immune-based biomarker signature is associated with mortality in COVID-19 patients. JCI Insight [Internet]. 2021;6. Available from: https://doi.org/10.1172/jci.insight.144455

42. Vanderbeke L, Van Mol P, Van Herck Y, De Smet F, Humblet-Baron S, Martinod K, et al. Monocyte-driven atypical cytokine storm and aberrant neutrophil activation as key mediators of COVID-19 disease severity. Nat Commun [Internet]. 2021;12:4117. Available from: https://doi.org/10.1038/s41467-021-24360-w

43. Hubbard AK, Rothlein R. Intercellular adhesion molecule-1 (ICAM-1) expression and cell signaling cascades. Free Radic Biol Med. 2000;28:1379–86.

664 44. Bui TM, Wiesolek HL, Sumagin R. ICAM-1: A master regulator of cellular responses in
665 inflammation, injury resolution, and tumorigenesis. J Leukoc Biol. 2020;108:787–99.

666 45. Bernatchez SF, Atkinson MR, Parks PJ. Expression of intercellular adhesion molecule-1 on
667 macrophages in vitro as a marker of activation. Biomaterials. 1997;18:1371–8.

668 46. Zhong H, Lin H, Pang Q, Zhuang J, Liu X, Li X, et al. Macrophage ICAM-1 functions as a
669 regulator of phagocytosis in LPS induced endotoxemia. Inflammation Research [Internet].
670 2021;70:193–203. Available from: https://doi.org/10.1007/s00011-021-01437-2

671 47. Wiesolek HL, Bui TM, Lee JJ, Dalal P, Finkielsztein A, Batra A, et al. Intercellular
672 Adhesion Molecule 1 Functions as an Efferocytosis Receptor in Inflammatory Macrophages.
673 Am J Pathol [Internet]. 2020;190:874–85. Available from:
674 https://www.sciencedirect.com/science/article/pii/S0002944020300213

675 48. de Pablo R, Monserrat J, Reyes E, Díaz D, Rodríguez-Zapata M, de la Hera A, et al.
676 Circulating sICAM-1 and sE-Selectin as biomarker of infection and prognosis in patients with
677 systemic inflammatory response syndrome. Eur J Intern Med. 2013;24:132–8.

678 49. Yoshida H, Hunter CA. The Immunobiology of Interleukin-27. Annu Rev Immunol
679 [Internet]. 2015;33:417–43. Available from: https://doi.org/10.1146/annurev-immunol-
680 032414-112134

681 50. Yoshida H, Nakaya M, Miyazaki Y. Interleukin 27: a double-edged sword for offense and
682 defense. J Leukoc Biol [Internet]. 2009;86:1295–303. Available from:
683 https://doi.org/10.1189/jlb.0609445

684 51. Morita Y, Masters EA, Schwarz EM, Muthukrishnan G. Interleukin-27 and Its Diverse
685 Effects on Bacterial Infections. Front Immunol [Internet]. 2021;12. Available from:
686 https://www.frontiersin.org/articles/10.3389/fimmu.2021.678515

687 52. Hanna WJ, Berrens Z, Langner T, Lahni P, Wong HR. Interleukin-27: a novel biomarker in
688 predicting bacterial infection among the critically ill. Crit Care [Internet]. 2015;19:378.
689 Available from: https://doi.org/10.1186/s13054-015-1095-2

690 53. Pot C, Apetoh L, Awasthi A, Kuchroo VK. Molecular pathways in the induction of
691 interleukin-27-driven regulatory type 1 cells. J Interferon Cytokine Res. 2010;30:381–8.

692 54. Bosmann M, Ward PA. Modulation of inflammation by interleukin-27. J Leukoc Biol.
693 2013;94:1159–65.

694 55. Luster A, Ravetch J. Biochemical characterization of a gamma interferon-inducible
695 cytokine (IP-10). J Exp Med. 1987;166:1084–97.

696 56. Neville LF, Mathiak G, Bagasra O. The immunobiology of interferon-gamma inducible
697 protein 10 kD (IP-10): a novel, pleiotropic member of the C-X-C chemokine superfamily.
698 Cytokine Growth Factor Rev. 1997;8:207–19.

699 57. Madhurantakam S, Lee ZJ, Naqvi A, Prasad S. Importance of IP-10 as a biomarker of host
700 immune response: Critical perspective as a target for biosensing. Curr Res Biotechnol
701 [Internet]. 2023;5:100130. Available from:
702 https://www.sciencedirect.com/science/article/pii/S2590262823000126

703 58. Liu M, Guo S, Hibbert JM, Jain V, Singh N, Wilson NO, et al. CXCL10/IP-10 in infectious
704 diseases pathogenesis and potential therapeutic implications. Cytokine Growth Factor Rev.
705 2011;22:121–30.

706 59. Lee EY, Lee Z-H, Song YW. CXCL10 and autoimmune diseases. Autoimmun Rev.
707 2009;8:379–83.

708 60. Shi L, Westerhuis JA, Rosén J, Landberg R, Brunius C. Variable selection and validation
709 in multivariate modelling. Bioinformatics [Internet]. 2019;35:972–80. Available from:
710 https://doi.org/10.1093/bioinformatics/bty710

711

Figures

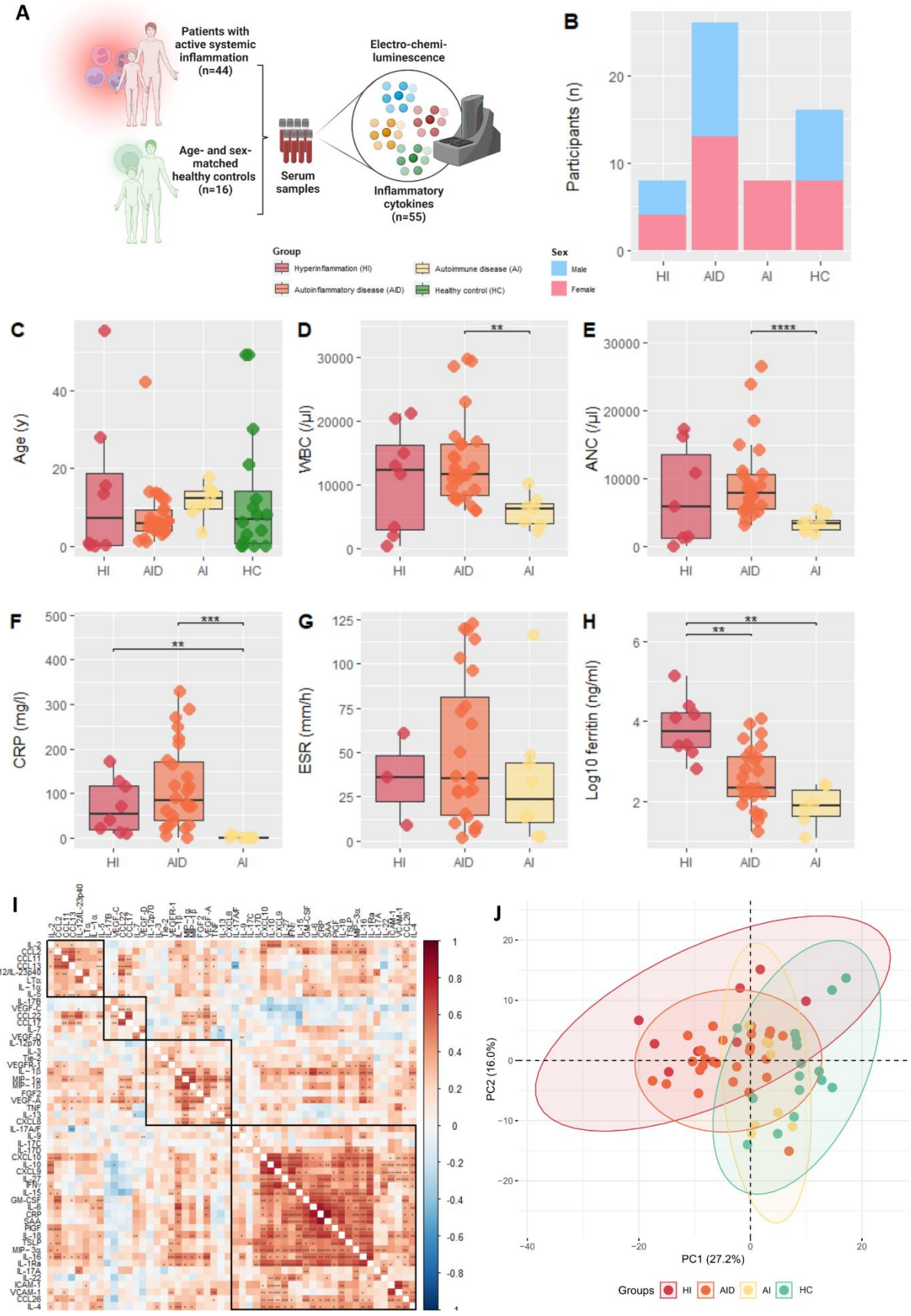
A
Patients with active systemic inflammation (n=44)
Age- and sex-matched healthy controls (n=16)
Serum samples
Electro-chemi-luminescence
Inflammatory cytokines (n=55)
Group
Hyperinflammation (HI)
Autoinflammatory disease (AID)
Autoimmune disease (AI)
Healthy control (HC)
Sex
Male
Female
B
Participants (n)
HI
AID
AI
HC
C
Age (y)
D
WBC (/μl)
E
ANC (/μl)
F
CRP (mg/l)
G
ESR (mm/h)
H
Log10 ferritin (ng/ml)
I
J
PC1 (27.2%)
PC2 (16.0%)
Groups

Figure 1: ***Fig 1A:*** *Outline of the study, including the number of participants and quantified cytokines.* ***Fig 1B-H:*** *Stacked bar chart and box-and-whisker plots showing demographic parameters for patients and healthy individuals and routine laboratory investigations in patients subjected to multiplex protein quantification. Statistical significance was calculated using the Wilcoxon signed-rank test between groups of continuous data or Pearson's chi-squared test for differences in sex proportions (only B-H adjusted p-values <0.05 are shown and are indicated by *, P < 0.05; **, P < 0.01; and ***, P < 0.001.* ***Fig 1I:*** *Spearman correlation plot of normalized signal intensity (log2FC as compared to median of HCs) for each biomarker from patients; B-H adjusted p-values are hierarchically clustered and indicated by *, P < 0.05; **, P < 0.01; and ***, P < 0.001; the color of the squares represents the absolute value of the corresponding Spearman rho values. Four clusters based on hierarchical closeness are denoted in black rectangles.* ***Fig 1J:*** *First two components (PC1 and PC2) of the principal component analysis of all normalized biomarkers from patients; 95% confidence interval ellipses are shown for each group. The percentage of explained variance is denoted in the axes. Abbreviations used: hyperinflammation (HI), autoinflammatory disease (AID), systemic autoimmune disease (AI), healthy control (HC), white blood cell (WBC) counts, absolute neutrophil count (ANC), C-reactive protein (CRP), erythrocyte sedimentation rate (ESR)*

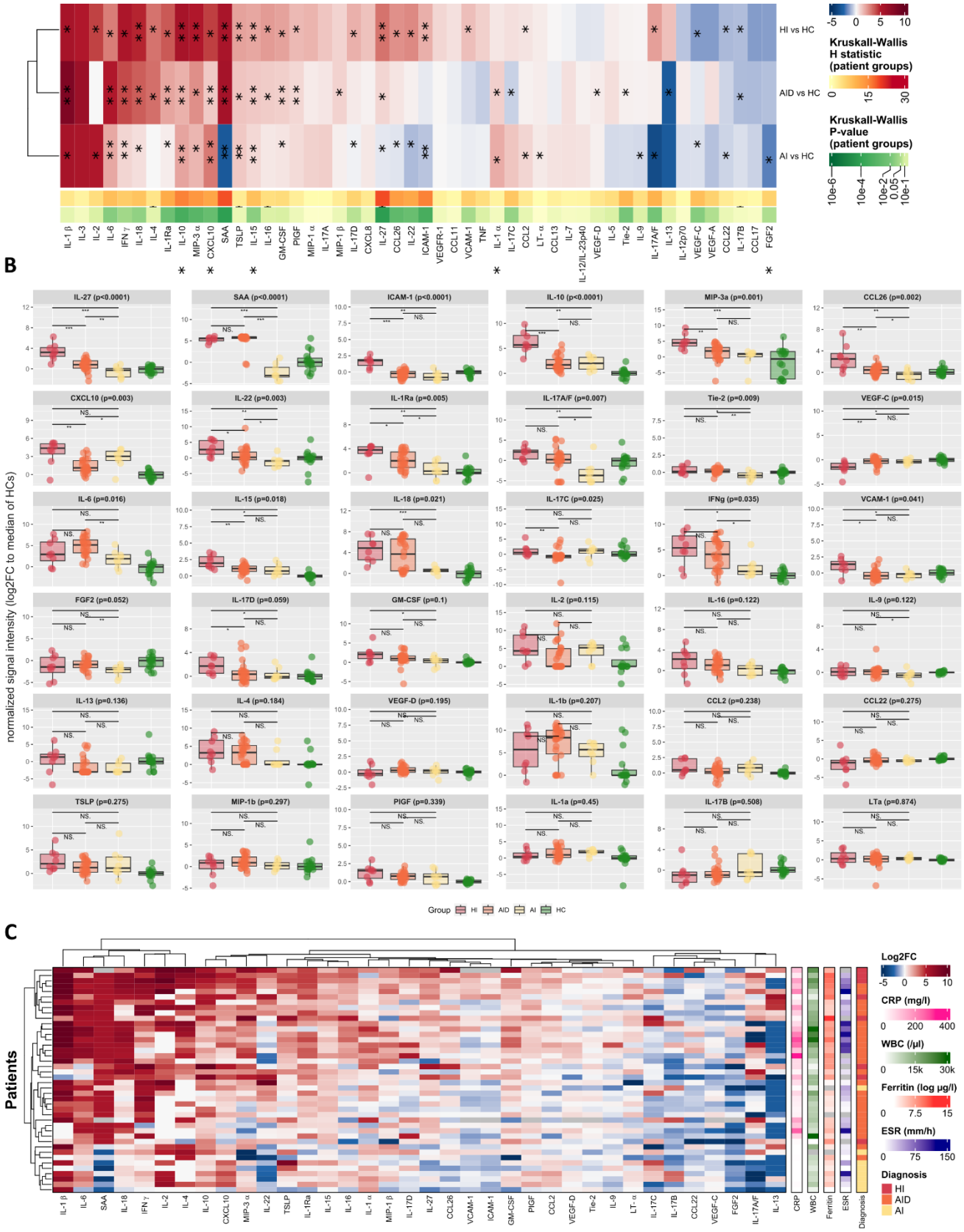
HI vs HC
AID vs HC
AI vs HC
Kruskall-Wallis H statistic (patient groups)
Kruskall-Wallis P-value (patient groups)
IL-1 β IL-3 IL-2 IL-6 IFN γ IL-18 IL-4 IL-1Ra IL-10 MIP-3 α CXCL10 SAA TSLP IL-15 IL-16 GM-CSF PlGF MIP-1 α IL-17A MIP-1 β IL-17D CXCL8 IL-27 CCL26 IL-22 ICAM-1 VEGFR-1 CCL11 VCAM-1 TNF IL-1 α IL-17C CCL2 LT - α CCL13 IL-7 IL-12/IL-23p40 VEGF-D IL-5 Tie-2 IL-9 IL-17A/F IL-13 IL-12p70 VEGF-C VEGF-A CCL22 IL-17B CCL17 FGF2
B
IL-27 (p<0.0001)
SAA (p<0.0001)
ICAM-1 (p<0.0001)
IL-10 (p<0.0001)
MIP-3a (p=0.001)
CCL26 (p=0.002)
CXCL10 (p=0.003)
IL-22 (p=0.003)
IL-1Ra (p=0.005)
IL-17A/F (p=0.007)
Tie-2 (p=0.009)
VEGF-C (p=0.015)
IL-6 (p=0.016)
IL-15 (p=0.018)
IL-18 (p=0.021)
IL-17C (p=0.025)
IFNg (p=0.035)
VCAM-1 (p=0.041)
FGF2 (p=0.052)
IL-17D (p=0.059)
GM-CSF (p=0.1)
IL-2 (p=0.115)
IL-16 (p=0.122)
IL-9 (p=0.122)
IL-13 (p=0.136)
IL-4 (p=0.184)
VEGF-D (p=0.195)
IL-1b (p=0.207)
CCL2 (p=0.238)
CCL22 (p=0.275)
TSLP (p=0.275)
MIP-1b (p=0.297)
PlGF (p=0.339)
IL-1a (p=0.45)
IL-17B (p=0.508)
LTa (p=0.874)
normalized signal intensity (log2FC to median of HCs)
Group HI AID AI HC
C
Patients
Log2FC
CRP (mg/l)
WBC (/µl)
Ferritin (log µg/l)
ESR (mm/h)
Diagnosis
HI
AID
AI
IL-1 β IL-6 SAA IL-18 IFN γ IL-2 IL-4 IL-10 CXCL10 MIP-3 α IL-22 TSLP IL-1Ra IL-15 IL-16 IL-1 α MIP-1 β IL-17D IL-27 CCL26 VCAM-1 ICAM-1 GM-CSF PlGF CCL2 VEGF-D Tie-2 IL-9 LT - α IL-17C IL-17B CCL22 VEGF-C FGF2 IL-17A/F IL-13
CRP WBC Ferritin ESR Diagnosis

728

Figure 2: ***Fig 2A:*** *Hierarchically clustered heatmap showing the median log2FC differences between patient groups versus healthy controls (HC). Unadjusted P-values by Mann-Whitney U test are indicated by *, P < 0.05; **, P < 0.01; and ***, P < 0.001. The bottom annotation shows the H statistic and P-values of test all variables between all disease groups (without HCs, unadjusted P-values by Kruskal-Wallis test).* ***Fig 2B:*** *Box-and-whisker plots showing normalized signal intensities in patients and HC (log2 fold change to the median of age-matched healthy controls). Only cytokines with significant differences among patient groups (unadjusted P-values <0.05 by Kruskal-Wallis test, indicated in the labels) or when comparing each patient group with HCs (unadjusted P-values by Mann-Whitney U test are indicated by *, P < 0.05; **, P < 0.01; and ***, P < 0.001) are presented. Cytokines with no significant differences are shown in Fig S2A.* ***Fig 2C:*** *Hierarchically clustered heatmap showing normalized individual patient data for biomarkers with significant differences (related to Fig 2B). Missing values (n=12) were imputed by missMDA using an iterative PCA algorithm. The labeling of patient groups and routine laboratory measurements for each individual are shown in the right annotation. Abbreviations used: hyperinflammation (HI), autoinflammatory disease (AID), systemic autoimmune disease (AI), healthy control (HC), white blood cell (WBC) counts, C-reactive protein (CRP), erythrocyte sedimentation rate (ESR)*

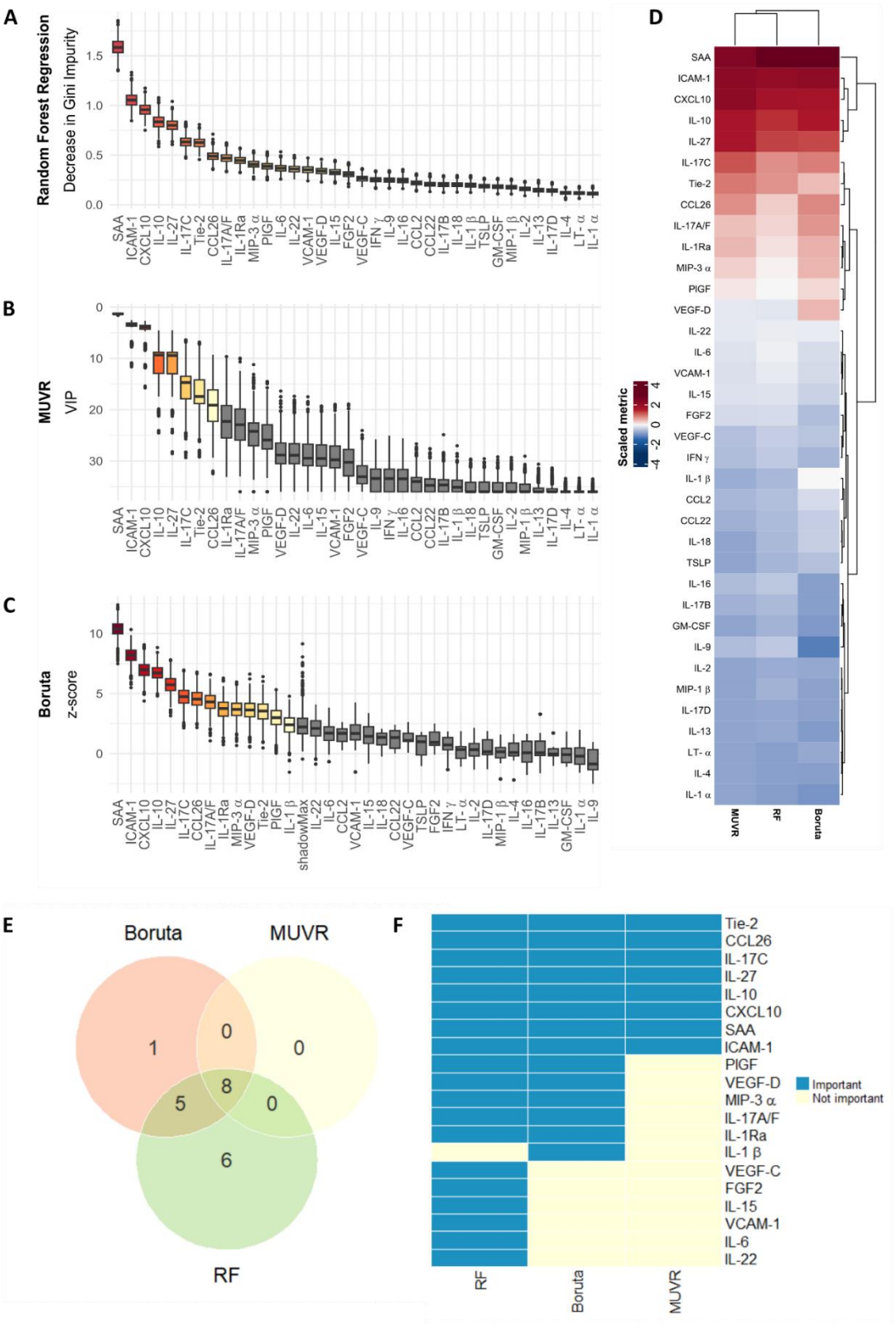

743

744 *Figure 3:* ***Fig 3A-C:*** *Results of repeated runs (1000x) of machine learning methods applied to 36 cytokines (input) with patient*
745 *groups as outcome variables. Box-and-whisker plots are ranked based on the median of the corresponding metric. For Random*
746 *Forest (RF) regression, the decrease in Gini Impurity is shown (A). For Multivariate methods with Unbiased Variable Selection*

in R (MUVR), the variable importance of projection (VIP) is plotted on an inverse scale (B). Biomarkers selected using the "all-relevant" model are colored. For Boruta, the z-score of the Mean Decrease in Accuracy is shown, whereby variables with a median z-score higher than the maximum shadow attributes are colored (C). ***Fig 3D:*** *Hierarchically clustered heat map showing the median scaled metrics for each cytokine and each algorithm used (related to Fig 3A-C).* ***Fig 3E:*** *Venn diagram of cytokines selected as important by each algorithm (i.e., being present in the top half of RF, the all-relevant selection of MUVR, and scoring higher than the maximum shadow attributes in Boruta).* ***Fig 3F:*** *Heatmap showing which cytokines were selected as important by each algorithm (related to Fig 3E)*

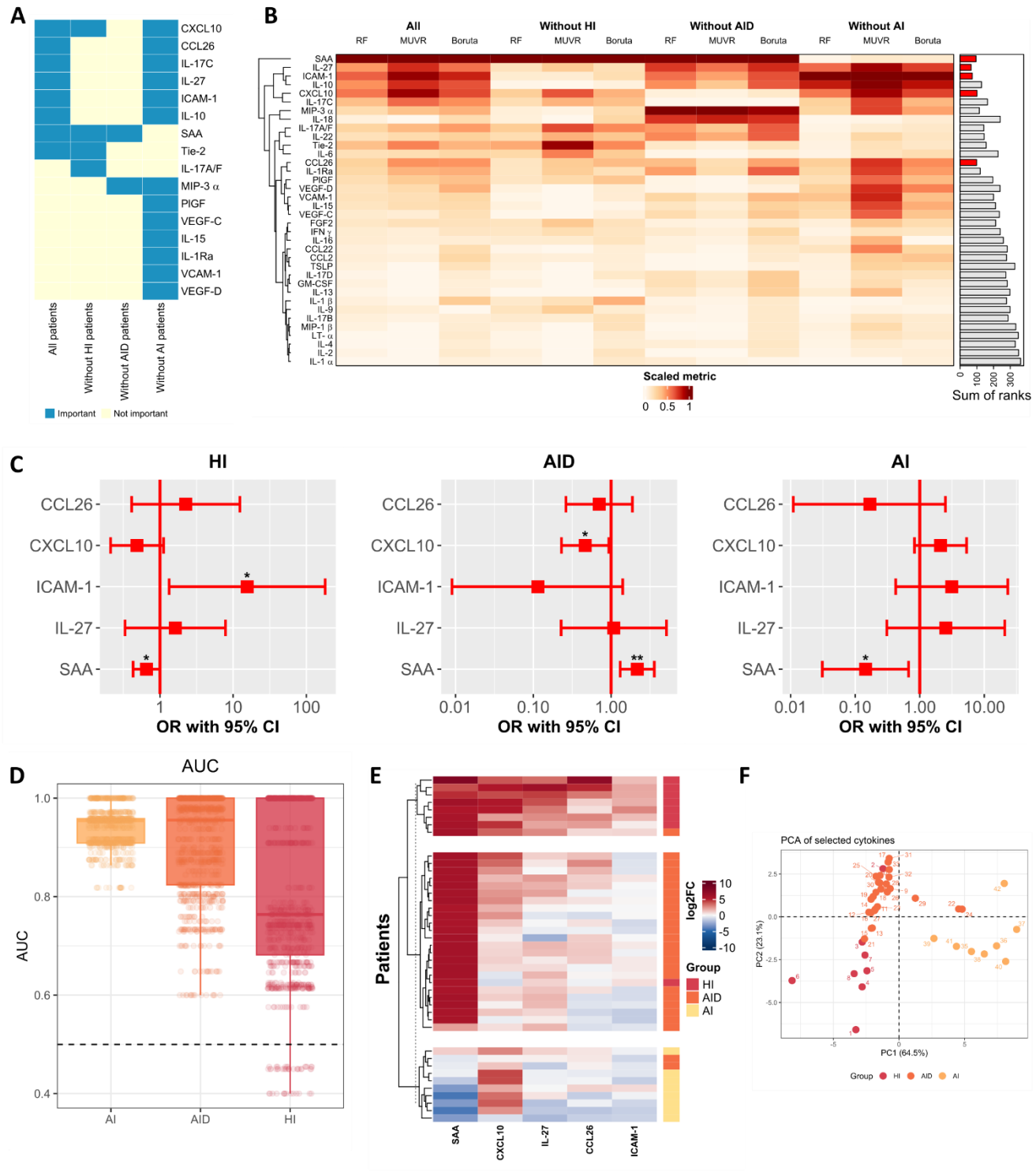

Figure 4: ***Fig 4A:*** *Heatmap showing the summary of which cytokines were selected as important by every algorithm (RF, MUVR, and Boruta) depending on which dataset was used (the original analysis on all patients or the sensitivity analyses on filtered patient sets).* ***Fig 4B****: Hierarchically clustered heatmap showing the median scaled metrics for each cytokine, each algorithm, and dataset used, including filtered datasets without patients presenting with hyperinflammation (HI), without autoinflammatory diseases (AID), or without systemic autoimmune disease (AI). The annotation on the right shows the sum of the rankings for each cytokine across all analyses. The five cytokines with the lowest ranks are shown in red.* ***Fig 4C:*** *Forest*

*plots of adjusted odds ratios (OR) and 95% confidence intervals (CI), presented on a logarithmic scale, as calculated by binomial logistic regression using the five prioritized cytokines as input and the disease groups (HI, AID, and systemic AI) as outcomes. Denoted P-values concern the model and were calculated using Chi-square test. P-values of each variable were calculated using the Wald test and are indicated by *, P < 0.05; and **, P < 0.01.* ***Fig 4D:*** *Box-and-whisker plots of repeated calculation (1000x) of the area under the curve (AUC) with random generation of training and test sets of the five prioritized cytokines (CCL26, CXCL10, ICAM-1 IL-27, and SAA) and predicting the diagnosis using logistic regression modelling.* ***Fig 4E:*** *Hierarchically clustered heatmap showing normalized patient data of selected cytokines and k-means partitioning in three clusters with the known diagnoses color-coded in the annotation on the right.* ***Fig 4F:*** *First two components (PC1 and PC2) of principal component analysis (PCA) of the five prioritized cytokines (CCL26, CXCL10, ICAM-1 IL-27, and SAA) of patients; label colors and numbers denote patients' known diagnosis and identification, as presented in Supplementary data, respectively. Percentage of explained variance is denoted in the axes labels.*

Tables

	All patients	HI	AID	Systemic AI	P-value	HCs
n	44	9	27	8		16
Age (y), median (IQR)	6.5 [3.76, 13.33]	11 [0.28, 15.61]	5.9 [3.84, 9.29]	12.4 [9.67, 14.08]	0.123	7.0 (0.8, 14.3)
Female sex, n (%)	26 (59.1)	5 (55.6)	13 (48.1)	8 (100.0)	**0.031**	8 (50)
WBC (/µl), median (IQR)	10960 [7045, 15590]	12890 [3370, 20320]	11500 [8610, 16340]	6240 [3935, 7040]	**0.013**	
ANC (/µl), median (IQR)	6060 [3845, 10620]	8347.50 [1324.25, 16473.25]	7390 [5452, 10620]	3393 [2465, 3927.50]	**0.005**	
CRP (mg/l), median (IQR)	69.3 [11.17, 141.93]	69.6 [20.40, 127.10]	88.4 [42.65, 175.75]	0 [0, 1.40]	**<0.001**	
Ferritin (µg/l), median (IQR)	478.5 [120, 2480.75]	12241 [2468, 21425]	215 [131, 1281]	78.5 [43.75, 206.25]	**<0.001**	
ESR (mm/h), median (IQR)	35.5 [13.75, 73.75]	48.5 [29.25, 70]	35.5 [14.75, 81]	23.5 [10.25, 44.25]	0.522	
Systemic steroid use, n (%)	8 (18.2)	5 (55.6)	3 (11.1)	0 (-)	**0.004**	
Biological therapy, n (%)	2 (4.5)	2 (22.2)	0 (-)	0 (-)	0.017	

Table 1: *Demographic and routine laboratory data of patients and healthy controls (HC) included in the study. P-values were calculated using the Kruskal-Wallis test for continuous variables and Fisher's Exact test for proportional data between patients with hyperinflammation (HI), autoinflammatory disease (AID) and systemic autoimmune disease (AI).*

Supplementary data

Top 25 correlations

	Variable	Variable	Spearman rho	Adjusted P-value
1	SAA	CRP	0.867738	3.43E-17
2	IL-6	CRP	0.801299	3.95E-09
3	CXCL9	IL-10	0.758571	7.41E-13
4	CXCL9	IFNγ	0.733366	8.75E-07
5	IL-1Ra	IL-16	0.713925	3.67E-08
6	VCAM-1	ICAM-1	0.712235	3.96E-08
7	IL-18	CRP	0.702404	4.79E-06
8	SAA	IL-6	0.692139	3.71E-06
9	SAA	IL-18	0.690477	7.16E-06
10	IL-6	IL-1β	0.677583	3.63E-07
11	CXCL10	IL-10	0.675577	1.07E-07
12	MIP-1β	MIP-1α	0.674921	2.07E-11
13	CXCL9	CXCL10	0.674921	6.81E-10
14	GM-CSF	CRP	0.659113	0.001102
15	IL-1Ra	IL-15	0.656874	2.36E-07
16	IL-1Ra	CRP	0.654819	1.60E-06
17	IL-18	IL-10	0.65184	0.00111
18	CCL17	CCL22	0.647421	2.06E-10
19	IL-6	GM-CSF	0.641103	0.000124
20	IL-15	IL-10	0.63692	6.85E-05
21	TSLP	IL-18	0.630645	0.007167
22	CXCL10	IL-1Ra	0.630564	8.70E-06
23	PlGF	CRP	0.63028	0.001427
24	PlGF	IL-6	0.629375	2.63E-05
25	IL-10	IFNγ	0.62922	1.87E-05

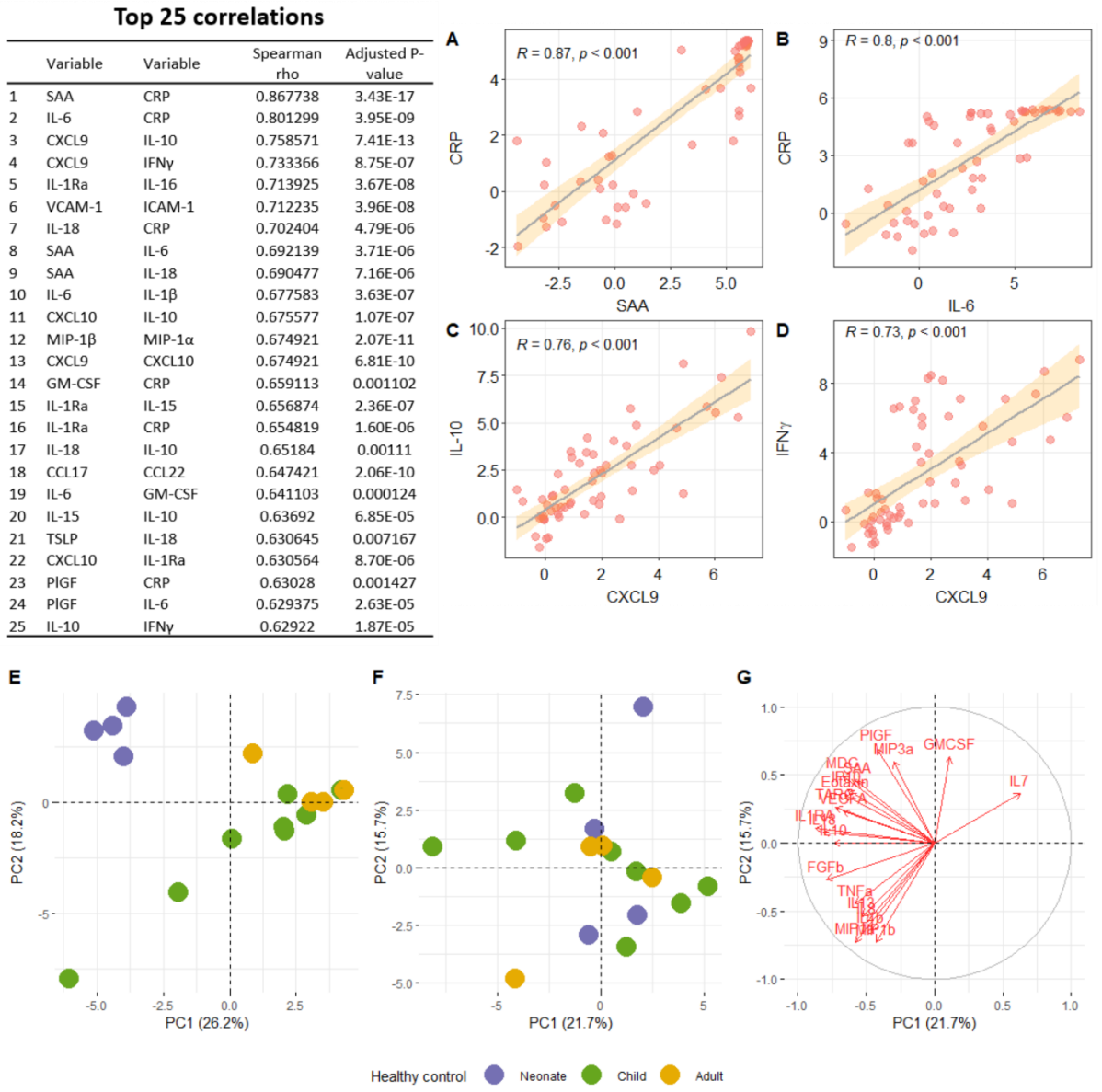

Figure S1: ***Fig S1A-D:*** *Pairs of normalized biomarkers with the highest correlation as calculated by Spearman rho. Individual data points for patients and B-H adjusted P-values are shown. 95% confidence interval (yellow shade) around the regression line (grey) as determined by linear regression is shown.* ***Fig S1E-F:*** *First two components (PC1 and PC2) of principal components analysis of raw data (E) and normalized biomarkers (F) from healthy controls by age group (infants: <12 months, children 1-18y, adults 21-49y). Percentage of explained variance is denoted in the axes labels.* ***Fig S1G:*** *Factor map of 20 most contributing variables to the first two components of normalized biomarker PCA (related to Fig S1F). Abbreviations used: principal component (PC)*

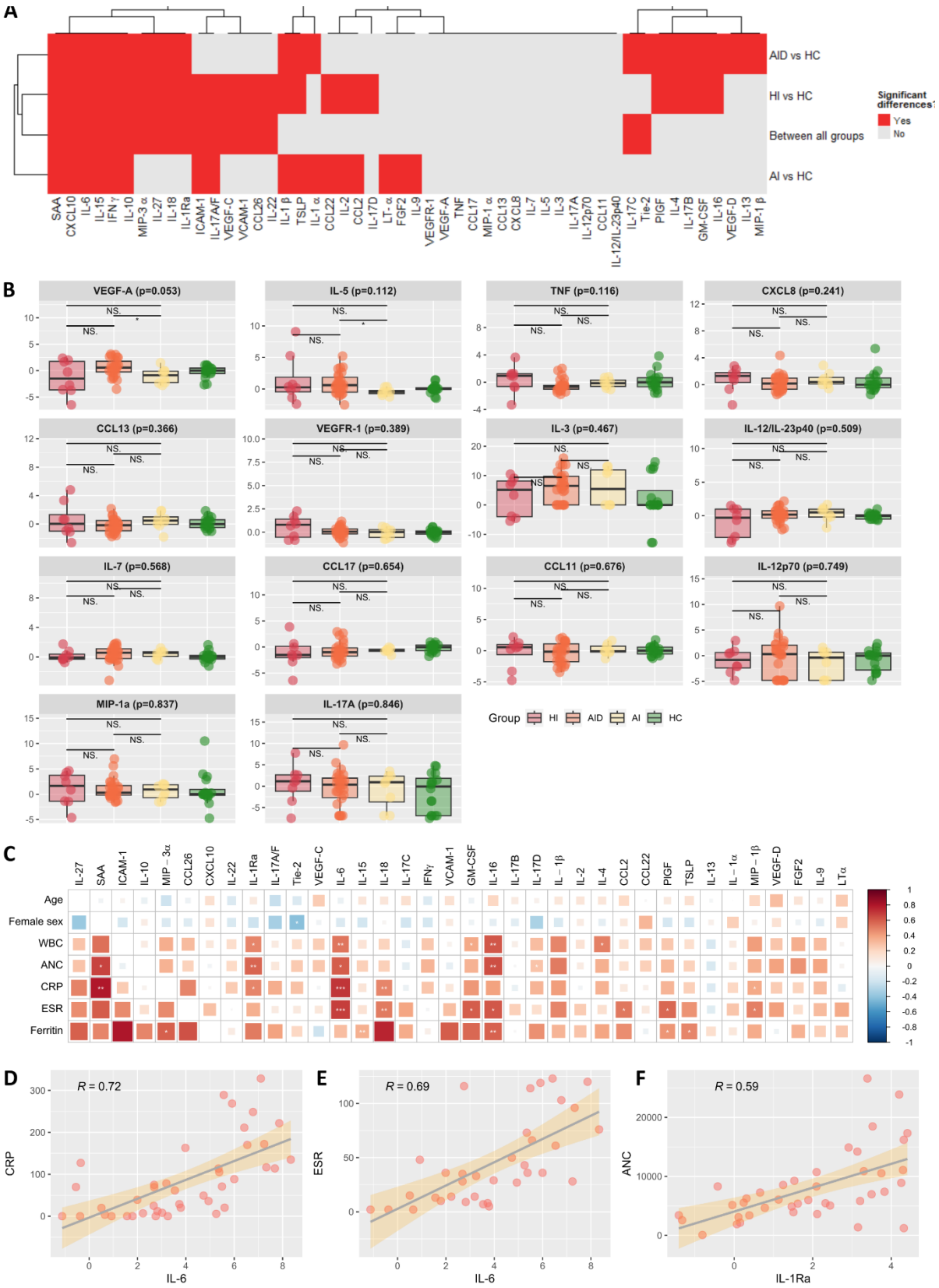

Figure S2: ***Fig S2A:*** *Hierarchically clustered heatmap showing the presence or absence of significant differences between groups of patients versus healthy controls (using unadjusted P-value <0.05 with Mann-Whitney U test) or among all three groups of patients (unadjusted P-value <0.05 using Kruskal Wallis test between HI, AID, and AI).* ***Fig S2B****: Box-and-whisker*

*plots showing the log2FC for patients and healthy controls (HCs) of cytokines without significant differences among patient groups or when comparing patient groups with HCs. Unadjusted P-values <0.05 by Kruskal-Wallis test among all disease groups are indicated in the labels. Unadjusted P-values by Mann-Whitney U test between each disease group and HCs are indicated below the comparison lines by *, P < 0.05; **, P < 0.01; and ***, P < 0.001.* ***Fig S2C:*** *Spearman correlation plot of normalized signal intensity (log2FC as compared to median of HCs) for selected biomarkers and demographic and routine laboratory data of patients; B-H adjusted p-values are hierarchically clustered and indicated by *, P < 0.05; **, P < 0.01; and ***, P < 0.001; the colour of the squares represent the absolute value of corresponding Spearman rho values.* ***Fig S2D-F:*** *Pairs of normalized biomarkers and their associated routine laboratory markers with the highest correlation as calculated by Spearman rho. Individual data points for patients and B-H adjusted P-values are shown. 95% confidence interval (yellow shade) around the regression line (grey) as determined by linear regression is shown. Abbreviations used: Hyperinflammation (HI), Autoinflammatory disease (AID), Autoimmunity (AI), Healthy control (HC), White blood cells (WBC), C-reactive protein (CRP), erythrocyte sedimentation rate (ESR)*

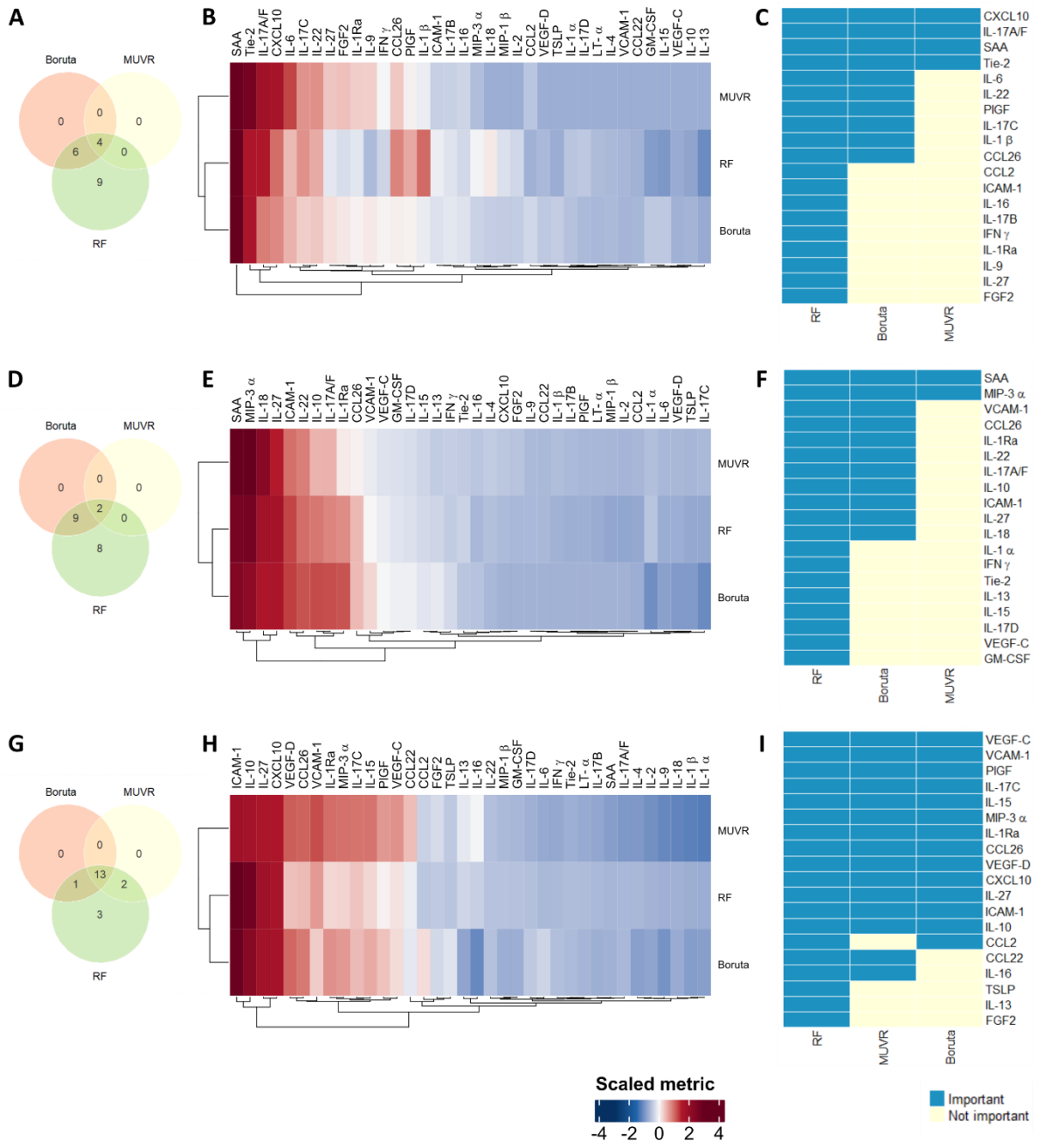

<u>Figure S3:</u> Results of sensitivity analyses using the same machine learning methods as presented in Figure 3 but whereby the data were filtered by consecutively leaving out one patient group. Results are presented, from top to bottom, for the analysis without patients presenting hyperinflammation (HI), without autoinflammatory diseases (AID) or without autoimmunity (AI). ***Fig S3A,D,G:*** *Venn diagram of cytokines selected as important by each algorithm (i.e., being present in the top half of RF, the all-relevant selection of MUVR and scoring higher than the maximum shadow attributes in Boruta).* ***Fig S3B,E,H:*** *Hierarchically clustered heatmap showing the median scaled metrics for each cytokine and each algorithm used.* ***Fig S3C,F,I:*** *Heatmaps showing which cytokines were selected as important (presence) by each algorithm (related to Fig 3S3A,D,G)*

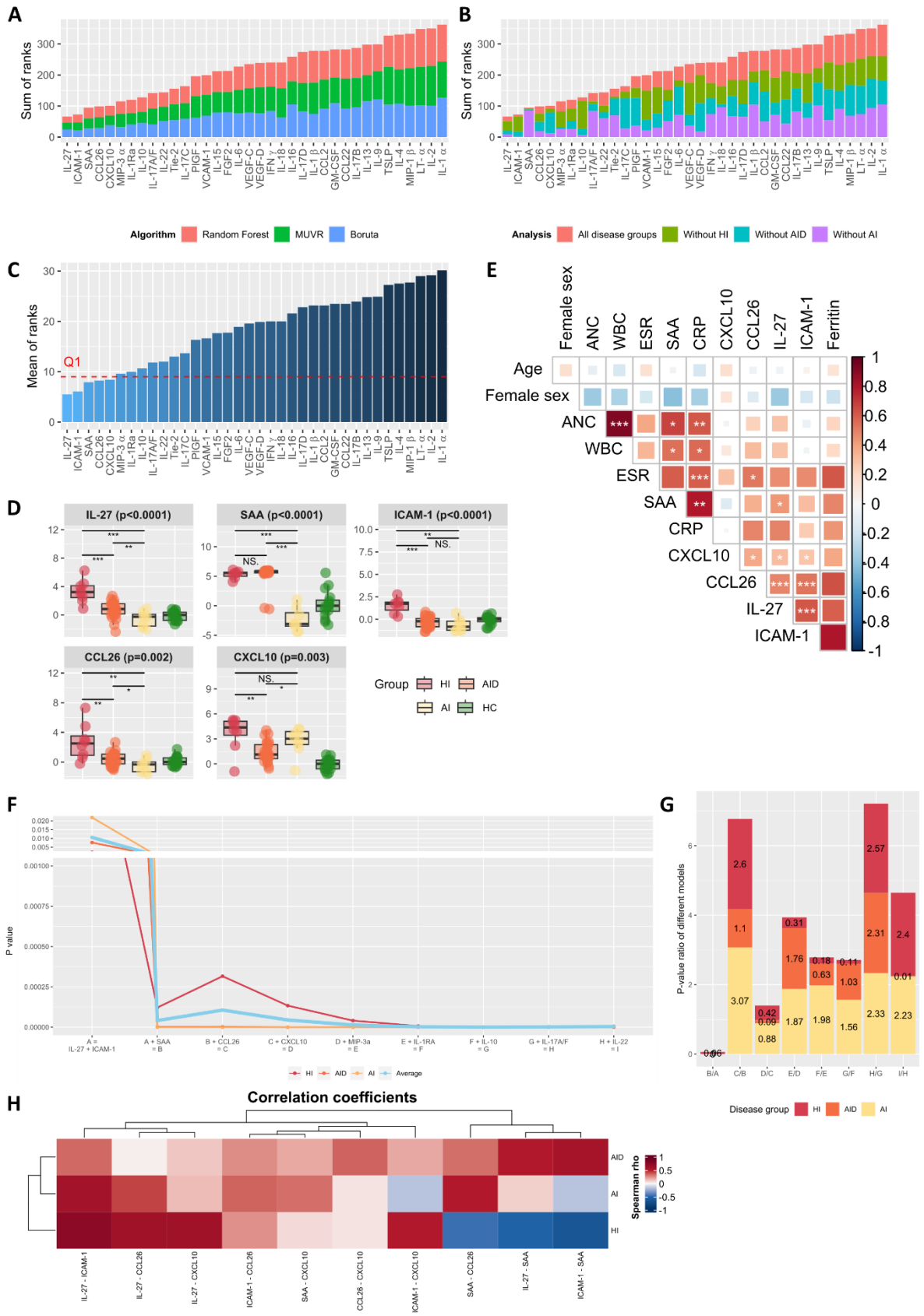

Figure S4: ***Fig S4A-C:*** *Ranking of cytokines as an importance metric to summarize machine learning methods with separate color coding for the sum of all ranks found by each algorithm (Fig S4A) and dataset used (Fig S4B), including filtered datasets*

without patients presenting hyperinflammation (HI), without autoinflammatory diseases (AID) or without autoimmunity (AI). The mean ranking across all analyses in shown in Fig S4C. The first quartile (Q1) of mean ranking is denoted. ***Fig S4D:*** *Box-and-whisker plots showing normalized signal intensity of prioritized cytokines. Unadjusted P-values <0.05 by Kruskal-Wallis test are indicated in the labels. Unadjusted P-values by Mann-Whitney U test between patient groups are indicated by *, P < 0.05; **, P < 0.01; and ***, P < 0.001. To compare, healthy control (HC) data is displayed, but, for clarity, P-values between patient groups and HCs are not presented here (these can be found in Fig. 2B or Fig. S2B).* ***Fig S4E:*** *Spearman correlation plot of normalized signal intensity (log2FC as compared to median of HCs) for prioritized cytokines, demographic variables and routine laboratory tests from patients; B-H adjusted p-values are hierarchically clustered and indicated by *, P < 0.05; **, P < 0.01; and ***, P < 0.001; the colour of the squares represent the absolute value of corresponding Spearman rho values.* ***Fig S4F:*** *Statistical significance of different logistic regression models and the average significance as calculated by chi square test. The prioritized cytokines are those incorporated in "D". The order of adding cytokines was based on the sum of ranks as presented in Fig S4A-C.* ***Fig S4G:*** *Fold change (ratio of P-values) of statistical significance of different logistic regression models as calculated by chi square test and color coded by patient group. The most prominent drop in P-value (ratios <1) occurred by adding SAA to IL-27 and ICAM-1 (= C model / B model) and after adding CXCL10 to the first four cytokines (= E model / D model).* ***Fig S4H:*** *Hierarchically clustered heatmap showing correlation between the five prioritized cytokines by patient group. The colour of the squares represent the absolute value of corresponding Spearman rho values. B-H adjusted p-values are denoted in each corresponding cell . Abbreviations used: Hyperinflammation (HI), Autoinflammatory disease (AID), Autoimmunity (AI), Healthy control (HC)*

	Demo-graphics		Diagnosis		Disease activity at sampling	Routine laboratory test at sampling					Therapy at sampling		
ID	Age (y)	Sex	Group	Specify	Describe	WBC (/µl)	ANC (/µl)	ESR (mm/u)	Ferritin (µg/l)	CRP (mg/l)	Steroids + dose	Biologics	Other
1	0.79	F	HI	primary HLH (UNC13D)	fever, pancytopenia, hepatosplenomegaly	1920	1359	*NA*	2519	69.6	Dexa 1.5mg/24h = 5mg/m²	-	antibiotics, blood transfusions
2	0.14	M	HI	primary HLH (PRF1)	fever > 10 days, pancytopenia, severe hepatomegaly	370	64	*NA*	2468	8.1	Dexa 5mg/m²/12h	-	ciclosporin, etoposide, antibiotics
3	0.01	M	HI	neonatal HLH - negative genetics	fever, hepatosplenomegaly, seizures, severe hepatitis, thrombocytopenia	14980	10875	*NA*	140949	20.4	-	-	antibiotics
4	0.28	M	HI	HLH - negative genetics	fever, hepatomegaly, erythematous skin rash, encephalopathy, crackled lips, skin desquamation, coagulopathy, thrombocytopenia, histiocytosis on bone marrow	12890	5820	*NA*	1674	127.1	Dexa 3.2mg/24h = 10mg/m²/24h	-	IVIG 48h before, antibiocs
5	55.27	F	HI	secondary HLH (EBV driven hepatosplenic T cell lymphoma)	fever, oral aphthosis, weight loss, liver histiocytosis, mediastinal adenopathy, EBV positive PCR in blood, ANA+, COVID+	3370	1220	9	12241	12.2	hydrocortison 15mg/24h	infliximab stop since 5 weeks	AZA stop since 2 weeks
6	15.61	F	HI	MAS, underlying sJIA (DD DRESS on sulfasalazine)	fever, myalgia, abdominal pain, erythematous skin rash, hemodynamic shock	21220	16191	*NA*	631	114	-	-	sulfasalazine, NSAIDs on demand
7	11.00	F	HI	MAS, underlying sJIA	fever > 10 days, salmon pink rash, arthralgia wrist and ankle	21000	19300	97	21425	253.9			NSAIDs
8	13.51	F	HI	Kikuchi syndrome (underlying sJIA)	fever, cervical adenopathy, myalgia, coagulopathy	20320	17320	61	14320	10	-	-	antibiotics

9	27.89	M	HI	MAS, underlying AOSD	fever, erythematous skin rash, polyarthralgia, thoracal pain, encephalopathy, seizures, bone marrow histiocytosis	11690	*NA*	36	23806	39.1	MP 64mg/24h, 5 day pulse MP 500mg/24h untill 72h before sampling	anakinra 100mg/24h, sarilumab latest 3 weeks before	colchicine 0.5mg/12h, antibiotics
10	12.07	F	AID	sJIA - NLRP3 VUS	relapsing-remitting fever, abdominal pain, headache, cervical adenopathy, erythematous rash on hands and legs	5880	5050	15	202	19.7	MP 10mg/24h	-	cyclosporine 70 mg/12h
11	7.27	F	AID	sJIA	fatigue, polyarthralgia	11810	9250	50	196	49.2	P 10 mg/24h = 0.5mg/kg/24h	-	NSAIDs, MTX 15 mg/w
12	13.59	M	AID	sJIA	prolonged fever, arthralgia knees, generalized urticaria	28590	23870	66	11833	289.2	-	-	antibiotics
13	9.00	M	AID	sJIA	fever >2 weeks, intermittent erythematous skin rash on legs, myalgia	7900	6960	123	4907	211.2	-	-	IVIG 2g/kg 48h before, antibiocs, LD ASA
14	5.99	M	AID	sJIA	8 days fever (in total >12 days), arthritis, pink rash (papular too)	17600	14890	103	1032	248.6	-	-	-
15	14.03	M	AID	sJIA	5 weeks fever, malaise, myalgia, arthralgia, pink rash, mild splenomegaly	16200	10720	114	1281	70.8	-	-	-
16	1.16	F	AID	sJIA	3 week fevers, rash since few months, likely arthritis hips, swollen hands/feet	29400	8293	76	2380	134.9	-	-	NSAIDs
17	6.06	F	AID	sJIA	fever 10d, maculopapular erythematous rash, ri wrist arthritis	22900	18464	>120	1259	221.8	-	-	NSAIDs
18	9.57	F	AID	sJIA	fever > 12 days, salmon pink rash, myalgia, PIP-arthritis	6600	6250	28	1753	69	-	-	-
19	4.77	F	AID	sJIA	persistent fever, arthritis both knees, shoulders, wrists	11460	7390	96	650	116.6	-	-	NSAIDs
20	12.19	F	AID	sJIA	fever over 10 days, muscle weakness, abdominal pain, arthritis ankles	5860	3080	119	555	268.8	-	-	NSAIDs, antibiotics
21	6.49	F	AID	sJIA	fever over 7 days, arthralgia shoulder, ankle, hip, throat pain, generalized erythematous skin rash	12640	10520	*NA*	3560	328.4	-	-	NSAIDs, antibiotics

22	2.84	M	AID	sJIA	generalized erythematous skin rash, spiking fever during 10 days, joint pains, morning stiffness	16480	8899	73	8503	113.7	-	-	NSAIDs
23	42.23	M	AID	AOSD	persistent fatigue, throat ache, subfebrile	7600	5140	2	402	3.4	-	-	NSAIDs, colchicine 0,5mg/12h
24	1.25	M	AID	NLRP3 GOF	fever, cervical adenopathy	10960	5980	28	134	172.1	-	-	azithromycine 3x/week, SCIG 0.15g/kg/week
25	3.66	F	AID	Blau syndrome	erythematous skin ichtyosis (arms and legs; biopsy shows non-caseating granulomatosis) with bodgy tenosynovitis at wrists and midfoot	14500	5530	10	45	0	-	-	-
26	13.26	M	AID	FMF	recurrent pain crises (abdominal, thoracal), fever	7950	4660	36	215	105.1	-	-	NSAIDs
27	3.41	F	AID	FMF	fever, generalized urticarial exanthema, abdominal pain	9500	3920	*NA*	*NA*	24.8	-	-	colchicine 1mg/12h
28	5.92	M	AID	PFAPA	fever, tonsillitis, cervical adenopathy	14180	11070	36	146	88.4	-	-	-
29	3.79	M	AID	PFAPA	fever since 5 days, tonsillitis, cervical adenopathy	9280	3770	*NA*	*NA*	179.4	MP 1mg/kg 1 dose 4 days before	-	-
30	5.16	M	AID	PFAPA	recurrent fever, throat pain, aphthosis, good response medrol	11500	8536	27	44	36.1	-	-	-
31	3.90	M	AID	PFAPA	recurrent fever with oral aphthosis and cervical adenopathy and inguinal adenopathy	10800	7250	29	172	163	-	-	-
32	6.44	M	AID	PFAPA	atypical PFAPA with recurrent fever, vomiting, abdominal pain, throat pain, cervical adenitis	16700	14200	35	131	74.8	-	-	colchicine
33	4.15	M	AID	PFAPA	recurrent fever with oral aphthosis, throat pain, cervical adenopathy	29700	26580	14	80	78.1	-	-	NSAIDs
34	1.89	F	AID	PFAPA	recurrent fever (5-7d) without symptoms initially but after time with oral apths and throat pain and good responsive towards steroids	12600	8290	7	17	61.3	-	-	-

35	5.73	F	AID	PFAPA	recurrent 2-3d fever (40), abdominal pain (coughing too today), later on throat pain and oral aphts, great response to steroids	9220	6060	5	32	20.3	-	-	-
36	4.27	F	AID	PFAPA	recurrent fever, 2-4 days, aphthosis, throat pain	8000	5374	8	54	28.8	-	-	-
37	11.07	F	AI	JDM	outspoken limb muscle weakness due to severe myositis, mild skin signs, later calcinosis	10100	5440	14	246	6.9	-	-	NSAIDs
38	17.79	F	AI	JDM	muscle pain, fatigue, little power, rash	6240	3610	48	70	0	-	-	-
39	3.57	F	AI	JDM	Gottron, muscle pain and less power, MRI normal	4180	2150	2	35	0	-	-	-
40	13.66	F	AI	SLE	AI hepatitis, arthritis elbow 3 days few weeks back	*NA*	3406	13	*NA*	0	-	-	-
41	13.86	F	AI	SLE	pericardial effusion, pleuritis, vasculitis skin, mild flexion contracture knees	3690	1880	43	*NA*	5.6	-	-	desloratadine
42	9.97	F	AI	scleroderma	polyarthritis, scleroderma	6590	3380	33	87	0	-	-	-
43	14.74	F	AI	scleroderma	polyarthritis, raynaud, scleroderma	7490	4880	116	261	0	-	-	-
44	8.77	F	AI	linear scleroderma	linear scleroderma finger since May 2020	2570	2570	2	12	0	-	-	-

Table S1: ***Demographic and clinical data of patients***